THE EFFECT OF HONEY ON SYNTHESIZED STARCH-SILVER NANOPARTICLES FOR THE INHIBITION OF MILD STEEL CORROSION IN ACID MEDIUM

BY

ANTHONY FERDINAND ESO EGBUNIWE

DEPARTMENT OF CHEMISTRY,

FALCULTY OF SCIENCE,

AHMADU BELLO UNIVERSITY,

ZARIA, NIGERIA

AUGUST, 2019

THE EFFECT OF HONEY ON SYNTHESIZED STARCH-SILVER NANOPARTICLES FOR THE INHIBITION OF MILD STEEL CORROSION IN ACID MEDIUM

BY

Anthony Ferdinand Eso EGBUNIWE,

B.Sc. (MAIDUGURI) 2014

P15SCCH8083

A THESIS SUBMITTED TO THE SCHOOL OF POSTGRADUATE STUDIES, AHMADU BELLO UNIVERSITY, ZARIA

IN PARTIAL FULFILLMENT OF THE REQUIREMENTS FOR THE AWARD OF MASTER DEGREE IN ANALYTICAL CHEMISTRY

DEPARTMENT OF CHEMISTRY,

FACULTY OF SCIENCE,

AHMADU BELLO UNIVERSITY,

ZARIA, NIGERIA

AUGUST, 2019

DECLARATION

I declare that the work in this project thesis entitled "THE EFFECT OF HONEY ON SYNTHESIZED STARCH-SILVER NANOPARTICLES FOR THE INHIBITION OF MILD STEEL CORROSION IN ACID MEDIUM" has been carried out by me in the Department of Chemistry. The information derived from previous literature has been duly acknowledged in the text and referenced accordingly. No part of this project thesis was previously presented for another degree or diploma at this or any other institution.

…….. …… ……..……..……

Name of Student Signature Date

CERTIFICATION

This project thesis titled "THE EFFECT OF HONEY ON SYNTHESIZED STARCH-SILVER NANOPARTICLES FOR THE INHIBITION OF MILD STEEL CORROSION IN ACID MEDIUM" by ANTHONY FERDINAND ESO EGBUNIWE meets the regulations governing the award of the award of the degree of M.Sc. Analytical Chemistry of the Ahmadu Bello University and approved for its contribution to knowledge and literary presentation.

Prof. P.A. Ekwumemgbo	…….	……...
Chairman, Supervisory Committee	Signature	Date
Dr. E.D. Paul	…….	……
Member, Supervisory Committee	Signature	Date
Prof. A. Uzairu	…….	…….
Head of Department	Signature	Date
Prof. S. A. Abdullahi	…….	……
Dean, Post Graduate School	Signature	Date

DEDICATION

This thesis is dedicated to God Almighty who gives strength to the weary and increases the power of the weak.

ACKNOWLEDGEMENT

My profound gratitude goes to my supervisory team, Prof. Patricia A. Ekwumemgbo and Dr. Elaoyi D. Paul, for their tolerance, patience, guidance and professional mentorship all through the course of my research. My sincere appreciation also goes to my lecturers for their moral and academic support.

I deeply appreciate my Mother, Matron (Mrs.) Francisca N. Egbuniwe for her unequivocal support during the course of my program. My siblings are not left out, as they have motivated and encouraged me in various ways. I am equally thankful to my colleagues for their intellectual supports and contribution in various ways.

Above all, I appreciate God Almighty for health, resources and sound mind.

ABSTRACT

In this research, the corrosion of mild steel was studied in acidic medium and the inhibitory effect as well as the synergism of starch-silver nanoparticles in combination with honey was evaluated. Synthesized starch-AgNPs was used to inhibit the corrosion of mild steel in acidic medium. The inhibition efficiency (%IE) for starch-AgNPs alone showed a maximum efficiency of 63.136% at 30^{o}C (200 mg/L) and a minimum efficiency of 19.900% at 70^{o}C (1 mg/L). However, the addition of 5 cm^{3} of honey further improved the inhibition efficiency. A maximum efficiency of 67.608% at 30^{o}C (200 mg/L) and a minimum efficiency of 29.914% at 70^{o}C (1 mg/L) was observed. Also, from the gravimetric data, a maximum and minimum corrosion rates of 52.467 mpy and 4.248 mpy at 70^{o}C and 30^{o}C respectively where observed, which is in contrast to the inhibition efficiency which decreased with increase in temperature. The FTIR analysis revealed the oxidation of the functional group present while, the UV-Visible analysis shows the complete reduction of Ag^{+} ions to Ag^{o} at an absorption peak of 415 nm.

TABLE OF CONTENT

LIST OF FIGURES

LIST OF APPENDIX

LIST OF PLATES

CHAPTER ONE

1.0 INTRODUCTION

Nanotechnology is the manipulation of matter on an atomic, molecular and super molecular scale (Drexler, 1986). Nanoscience has been established recently as a new interdisciplinary science. It can be defined as a whole knowledge on fundamental properties of nano-size objects (Sergeev, 2003; Sergeev, 2006). Nanotechnology is very diverse, ranging from extension of conventional device physics to completely new approaches based upon molecular self-assembly from developing new materials with dimension on the nanoscale to direct control of matter on the atomic scale (Frattini *et al*., 2005). In the United States, more than 4×10^6 tons of silver were consumed in 2000. Colloid silver is of particular interest because of distinctive properties such as good conductivity, chemical stability, catalytic and antibacterial activity (Frattini *et al*., 2005).

Buzea *et al.,* (2007), reported that nanoparticles involve particles that are within the scale of nanometer. Nanotechnology may be able to create many new materials and devices with a vast range of application, such as in medicine, electronics, biomaterials and energy production. Additional applications include molecular diagnostics and photonic devices, which take advantage of the novel optical properties of these nanomaterials. An increasingly common application is the use of silver nanoparticles for antimicrobial coatings, and many textiles, keyboards, wound dressings, and biomedical devices now contain silver nanoparticles that continuously release a low level of silver ions to provide protection against bacteria (Luo *et al.*, 2006).

Silver colloids are useful substrates for surface enhanced spectroscopy (SERS), since it partly requires an electrical conducting surface. Chemical reduction is the most frequently applied method for the preparation of silver nanoparticles (AgNPs) as stable colloidal dispersions in water or organic solvents (Vijayakumar *et al*., 2013). Silver nanoparticles have unique optical, electrical, and thermal properties and are being incorporated into products that range from photovoltaics to biological and chemical sensors (Zhang *et al*., 2016).

The use of corrosion inhibitors is one of the most practical methods for the protection of metals against corrosion, especially in acid media. The corrosion inhibitors are generally used to protect metals against the attack of the acid solutions, which are widely used in acid pickling, industrial cleaning, acid descaling, oil well acidizing, etc. (Popova *et al*., 2003; Ali *et al*., 2003).

Natural inhibitor substances are more attractive than synthesized organic inhibitors because they are environmentally friendly, nontoxic, cheap and readily available source of materials. In a "green" synthetic strategy, it is important to use nontoxic chemicals, environmentally benign solvents, and renewable materials (Ali *et al.*, 2003).

Starch is a natural polymer, available in abundance at low cost, renewable, and biodegradable. The packaging of amylose and amylopectin within the granules has been reported to vary among the starches from different species. The activity of the enzymes involved in starch biosynthesis may be responsible for the variation in amylose content among the various starches (Kossmann and Lloyd, 2000). The crystalline composition consists of around 15-45% of the starch granules. The crystalinity is exclusively associated with the amylopectin component, while the amorphous regions mainly represent amylose (Zobel *et al.*, 1988). Chemically, it is a polysaccharide carbohydrate consisting of a large number of glucose units joined together by

glycosidic bonds. The basic chemical formula of the starch molecule is $(C_6H_{10}O_5)_n$. The simplest form of starch is the linear polymer amylose; amylopectin is the branched form. Since, glucose exists in two forms: a straight chain and ring, as a straight chain, the molecule contains five -OH (hydroxyl) groups and one CH=O. (aldehyde) group. As a ring, the molecule still contains five hydroxyl groups, but its aldehyde group has been converted to a C-O-C (ether) group.

Chemical Structure of Glucose

Starch is produced by all green plants as an energy store. It is known to exhibit a very good performance as inhibitors for steel corrosion (Mobin *et al*., 2011). It inhibits the corrosion rate of mild steel to a considerable extent and is used as a protective agent because it is renewable and it can form dispersion in water. Starch is the predominant carbohydrate reserve in many plants; Starch is semicrystalline in nature with varying levels of crystallinity (Mobin *et al*., 2011).

The extent of crystallinity of native starch granules ranges from about 15% for high-amylose starches to about 45–50% for waxy starches. The granules have a hierarchical structure that can be observed readily by light and electron microscopy. The morphology of starch granules depends on the biochemistry of the chloroplast or amyloplast, as well as physiology of the plant (Singh *et al*., 2003). The granule is a partially crystalline material, i.e., within it, there are amorphous and crystalline regions and the degree of crystallinity is reported to be in the range 15-35% (Perez and Bertoft, 2010). The long range molecular order in the starch granules can be studied by the X-ray powder diffraction technique. Depending on the plant origin, native starch exhibits three different X-ray diffraction patterns. A-pattern, characteristic of cereal starches like wheat, barley, rye, oat, maize, rice, etc with characteristic d-spacing at 5.8, 5.2 and

3.8 Å, B-pattern characteristic of certain tuber and stem starches like potato which have characteristic d-spacing at 15.8, 5.9, 5.2, 4 and 3.7 Å and retrograded starch (Ring *et al*., 1988), and C-pattern, intermediate between A- and B-types which is found in legume starches and some tuber and seed starches (Perez and Bertoft, 2010). It has the characteristic d-spacing found in the A-pattern and the 15.8 Å d-spacing of the B-pattern (Zobel, 1988). The sharp diffraction patterns in the XRD are usually associated with crystalline material and the non-sharp areas with amorphous regions (Takeda *et al*., 1986).

Honey is a sweet food made from bees using nectars from flowers. Honey bees, transforms nectars into honey by a process of regurgitation, and stores it as a primary food source in wax honey combs inside the beehive. Honey gets it sweetness from the monosaccharide fructose and glucose, and has approximately the same sweetness as that of granulated sugar (Seeley, 2009). Honey belongs to the carbohydrate group of foods (sugars and starches), and is mainly a watery solution of two invent sugars: dextrose (glucose or grape sugar) and levulose (sucrose and fruit sugar), in nearly equal proportions (Bogdanov, 2012). Honey contains aromatic volatile oils which bestows it flavour, mineral elements: calcium, potassium, sodium, magnesium, iron, copper, phosphorous, etc. Ball (2007).

The main chemical components of honey (in percentages %) are:

Invert sugars 73.31

Sucrose (cane sugar) 2.63

Bextrin 2.89

Nitrogen substances 1.08

Water 18.98

Ash 0.24 (Ball, 2007)

Its specific gravity is 1.40 – 1.45, that is, it is heavier than water. Honey chelates and deactivates free ion, which would otherwise catalyze the formation of oxygen free radicals from hydrogen peroxide, leading to inflammation. The antioxidant constituents in honey help clean up oxygen free radicals present. The pH of honey is commonly between 3.2 – 3.5. This relative acidic pH level helps to prevent the growth of bacteria (Molan, 2001). A variety of ailments, from gastric disturbance to diabetic, ulcer, wounds and burns, through ingestion or topical application has been treated with honey. As an antibacterial agent, honey is used in treating a variety of ailment and this antibacterial properties are the result of the low water activity causing osmosis, chelating of free iron, it slow release of hydrogen peroxide, high acidity and the antibacterial activity of methylglyoxal (Wahdan, 1998). Honey has also been used for centuries as a treatment for sore throats, and coughs, and according to the recent research, maybe an effective soothing agent for coughs. Hydrogen peroxide formed in a slowly release manner by enzyme glucose oxidase present in honey renders it an antiseptic. Other uses of honey include: food in cooking, baking, as a spread on bread, as fragrance in soap and body lotions, and as sweeteners for various beverages (Mahmoud, 2012).

Mild steel is popular in the construction of different structures like pipelines, thermal chemical reactors and cooling systems, due to its recyclability, high life span, strength and ductility (Paul and Madunda, 2016). The corrosion of materials is one of the main problems facing industrial processes, generating huge financial losses. Metallic industrial structures such as mild steel are often exposed to conditions that facilitate corrosive processes (Mahgoub and Al-Rashdi, 2016).

Types of Corrosion

Electrochemical Corrosion Or Wet Corrosion

Evans (1960), established that underwater corrosion is essentially electrochemical in nature. When two dissimilar metals are contacted in an electrolyte, electrons pass through the metallic parts from anode to cathode while ions balance the charge by passing through the electrolyte in the reverse direction. In neutral or basic salt solutions, such as sea water, the accumulation of electrons in the cathode is counteracted by oxygen. Sea water induced corrosion is characteristic of both air saturated and electrolytic corrosion. Inherently, air saturated sea water is no more corrosive than air saturated fresh water. But the current of galvanic and concentration cells can flaw through greater distances in sea water and, therefore, the cathodic area of a cell may become relatively large, and the corrosion more intense. (Shaw, 1962).

This process is supported by aqueous solution in contact with the metal (forming an electrolyte) and the electrochemical process is closed by ion conduction through the electrolyte (Grundmeier *et al.*, 2000). This type of Corrosion occurs where a conducting liquid is in contact with the metal. This corrosion occurs due to the existence of separate anodic and cathodic parts, between which current flows through the conducting solution. At anodic area, oxidation reaction occurs thereby destroying the anodic metal either by dissolution or formation of compounds. Hence corrosion always occurs at anodic parts (Bradlee, 2003). Under certain conditions there are also other important cathodic reactions: the hydrogen evolution reaction, reduction of carbonic acid (H_2CO_3) (in oil and gas production), reduction of metal ions etc. The driving force for the electrochemical process (the corrosion) is the cell voltage, or in other words the potential difference between the anode and the cathode (Bradlee, 2003). In accordance with the conditions as described by the anodic and cathodic processes, the dissolution process is referred to as wet corrosion and the mechanism is typically electrochemical. In natural environments like

seawater, fresh water, soil and the atmosphere, oxygen reduction is the most dominant cathodic reaction (Little and Lee, 2007).

Direct Chemical Corrosion Or Dry Corrosion

There are three types of chemical Corrosion.

Corrosion due to other gases

This type of corrosion is due to gases like SO_2, CO_2, Cl_2, H_2S, F_2 etc. In this corrosion, the extent of corrosive effect depends mainly on the chemical affinity between the metal and the gas involved. The degree of attack depends on the formation of protective or non protective films on the metal surface (Reardon, 1995).

Oxidation corrosion or corrosion by oxygen

Oxidation Corrosion is brought about by the direct attack of oxygen at low or high temperature on metal surfaces in the absence of moisture. Alkali metals (Li, Na, K etc.,) and alkaline earth metals (Mg, Ca, Sn, etc.,) are rapidly oxidized at low temperature. At high temperature, almost all metals (except Ag, Au and Pt) are oxidized. When oxidation starts, a thin layer of oxide is formed on the metal surface and the nature of this film decides the further action (Yao *et al.,* 2000).

Liquid metal corrosion

This corrosion is due to chemical action of flowing liquid metal at high temperatures on solid metal or alloy. The corrosion reaction involves either dissolution of a solid metal by a liquid metal or internal penetration of the liquid metal into the solid metal. Eg. Coolant (sodium metal) leads to corrosion of cadmium in nuclear reactors (Yao *et al.,* 2000).

This type of Corrosion occurs mainly through the direct chemical action of atmospheric gasses like O_2, halogens, H_2S, SO_2, N_2 or anhydrous inorganic liquid with the metal surface. Dry

corrosion occurs in the absence of aqueous environment, usually in the presence of gases and vapours, mainly at high temperatures. The chemical corrosion is defined as the direct chemical attack of metals by the atmospheric gases present in the environment. (Madhankumar, 2012)

Underground or Soil Corrosion

The fundamental cause of the deterioration of pipeline buried underground is soil corrosion (Norin, 1998). Soil is a complex material, a porous heterogeneous and discontinuous environment constituted by mineral or organic solid phase, water liquid phase and air and other gas phase. Steel pipeline corrode in soil by complex electrochemical processes because of the presence different soil electrolytes. Underground corrosion is due to the corrosiveness of the soil. As the acidity of the soil increases, the rate of corrosion increases. In soils, water and gas occupy the spaces between solid particles, and these spaces can constitute as much as half the volume of dry soil. Some of this water is bound to mineral surfaces, whereas bulk water can flow through porous soil. Fluid flow through soil is controlled by the permeability of the soil, which, in turn, depends on the size distribution of the solid particles in the soil. Coarse – grained sand, for example, allows good drainage and access of atmospheric oxygen to a depth greater than, for example, fine - grained soils high in clay. Capillary action in fine - grained soil can draw water up, keeping the soil water - saturated, preventing drainage, retarding evaporation, and restricting oxygen access from the atmosphere to a buried structure, such as a pipeline (Wilmott and Jack, 2000).

The factors that influence corrosion in soil are numerous as soil type, moisture content and the position of the water table, soil resistivity, soluble ion content, soil pH, oxidation-reduction (redox) potential and the rates of microbes in soil corrosion (Rim-Rukeh and Awatefe, 2006). The electrochemical corrosion processes that take place on metal surfaces in soils occur in

the groundwater that is in contact with the corroding structure. Both the soil and the climate influence the groundwater composition. For example, some clay soils buffer the groundwater pH. Groundwater in desert regions can be high in chloride and very corrosive. On the other hand, groundwater in tropical climates tends to be very acidic. The corrosion behavior of iron and steel buried in the soil approximates, in some respects, the behavior on total immersion in water. Minor composition changes and structure of steel, for example, are not important to corrosion resistance. Hence, a copper – bearing steel, low alloy steel, mild steel, and wrought iron are found to corrode at approximately the same rate in any given soil. In addition, cold working or heat treatment does not affect the rate. Gray cast iron in soils, as well as in water, is subject to graphitic corrosion (Revie, 2008).

Pitting Corrosion

Pitting is one of the most complex and dangerous forms of metal corrosion (Kolotyrkin, 1963). Stainless steel is an attractive structural material because of its excellent corrosion resistance, which mainly depends on a thin passivating oxide film shielding the metal surface. However, this passivating layer is susceptible to localized pitting corrosion caused by aggressive anions such as those of chloride, which can rapidly lead to the damage or failure of structural components (Okamoto, 1973; Schweitzer, 2003; and Ramya, *et al*., 2010). Pitting corrosion is one of the most intensive forms of corrosion localized corrosion. Generally, pitting corrosion can be divided into two stages corresponding to initiation and the subsequent dissolution of the metal in a pit operating under stable conditions. A perforated cover over the pit mouth serves as a diffusion barrier together with the pit depth. Such pit covers are believed to be part of the original metal surface and contain many flaws such as small holes, which allow an ionic current to pass between the pit anolyte and the exterior electrolyte (Mankowski and Szklarska, 1975;

Ernst and Newman, 2002). Earlier works has suggested that the pit growth is controlled by diffusion within the occluded cell and within the metal salt layers present, which controls the corrosion current due to mass transport of the corrosion products out of the pit. Pitting starts at a certain critical potential known as the pitting potential (Kruger, 1976; Alvarez and Galvele, 1976; Szklarska-Smialowska, 1986; and Frankel, 1998). The disappearance of the pit covers is initiated by minor ruptures caused by osmotic pressure differences across the cover that are generated by the concentration difference between the pit anolyte and the exterior electrolyte (Frankel *et al.*,1987; Schwenk, 1964). When the pit is deep enough to serve as a sufficient diffusion barrier, the pit cover is no longer required, and stable pit growth is achieved. The pitting mechanism is complex, and the growth of metastable pits is often described as diffusion-controlled (Pistorius and Burstein, 1992).

General or Uniform Corrosion

This is probably the most common form of corrosion and can by characterized by chemical or electrochemical interaction between a metal and its environment with equivalent intensity over the entire exposed surface or over a large area. When handling chemical media in correlation with uniform corrosion, the metals involved can be classified into three groups in accordance with the rate of corrosion and the intended application as follows (Grundmeier *et al.*, 2000). General or uniform corrosion as the name implies occurs uniformly on the surface of the metal without any localization. It results in thinning or reduces the material and by visual inspection it can be detected. This is a very common form found in ferrous metals and alloys that are not protected by surface coating or inhibitors. A uniform layer of rust on the surface is formed when exposed to corrosive environments Atmospheric corrosion is a typical example of this type (Kolawole *et al*., 2016).

Atmospheric Corrosion

Recent atmospheric studies are based on a model established by Evans and Taylor (1972) and Stratmann and Streckel (1990). Atmospheric corrosion refers to corrosion in the air as opposed to corrosion that occurs in aqueous media. It is one of the most visible of all corrosion processes that is often seen on rusty bridges, flag poles, buildings and outdoor monuments. The exposure of a metal to the natural ambient atmosphere can vary considerably in terms of moisture content, temperature, and the amount of pollutants in air. Atmospheres are usually classified as rural, urban, industrial, marine, or a combination of these. Atmospheric corrosion is the most prevalent type of corrosion for common metals Naixin *et al* (2002).

It is based on wet–dry cycles that can be divided into three stages corresponding to variation of the electrolyte thickness on a determined period (day/night alternating, for example). By simulating wet–dry cycles on rusted coupons, Stratmann observed that during the first stage of the wet–dry cycle, the wetting period, the oxygen consumption is more important than the iron one. This author assumed that in this first stage, the anodic reaction of the corrosion process is the reduction of the lepidocrocite (FeOOH) present inside the corrosion layer. The reduced lepidocrocite is assumed to be conductive. This allows delocalising the cathodic reaction of reduction of the oxygen that occurs during the second period of the cycle, the wet one. Lastly, during the drying period the reduced lepidocrocite is reoxidised and a new cycle can start again (Neff *et al*., 2006). The large segment of the paint industry is committed to the manufacture and application of products for the protection of metals, as well as the large-scale operations of the galvanizing industry attest to the importance of controlling atmospheric corrosion (Roberge, 2008).

Galvanic Corrosion

When two dissimilar metals are electrically connected and exposed to an electrolyte, the metal higher in electrochemical series (low reduction potential) undergoes corrosion and the metal lower in electrochemical series (high reduction potential) is protected. This type of corrosion is called Galvanic corrosion. Galvanic corrosion can occur in multiphase alloys. The metal or alloy lower in the electrochemical series will become the anode and the noble one will become the cathode (Oldfield, 1988; Jones, 1996). Metal release rates of alloys should also be considered when evaluating the corrosion resistance. Metal release rates can give information about selective dissolution (Castle and Qiu 1990), which leads to an elemental enrichment on the alloy surface. For stainless steels, the selective dissolution results in chromium enriched surface (Castle and Qiu 1990; Herting *et al*. 2008). However an electrolytic connection between the metals and/or alloys, creating a closed electrical circuit is necessary for galvanic corrosion to occur (Noh *et al.,* 2000). Enrichment of chromium in the surface film is favourable for the corrosion resistance of stainless steels (Hong *et al*., 1996), resulting in an enhanced corrosion resistance of stainless steels (Bou-Saleh *et al*. 2007, Shahryari *et al.* 2007).

Crevice Corrosion

Crevice corrosion is a localized attack on a metal adjacent to the crevice between two joining surfaces (two metals or metal-nonmetal crevices). The corrosion is generally confined to one localized area to one metal. This type of corrosion can be initiated by concentration gradients due to ions or oxygen (Castle and Asami, 2004). Accumulation of chlorides inside crevices will aggravate damage. This is usually associated with a stagnant solution in a narrow gap or crevice which is formed under gaskets, washers, fastener heads, surface deposits and coatings (Shih *et*

al., 2004). If a crevice (a crack forming a narrow opening) between metallic and non-metallic materials is in contact with a liquid, the crevice becomes anodic region and undergoes corrosion. Hence, oxygen supply to the crevice is less. The exposed area has high oxygen supply and acts as cathode. Mechanism is similar to differential aeration (driven by changes in local chemistry of electrolyte), except that metal is initially passive (Kolawole *et al*., 2016).

Erosion Corrosion

This is as a result of the combined chemical attack and mechanical abrasion or wear along metal surface by eroding motion of fluid and/or its containing particles which is more detrimental to alloys that passivate by forming protective surface film. It is commonly found in piping, especially at bends, elbows, and abrupt changes in pipe diameter—positions where the fluid changes direction or flow suddenly becomes turbulent (Balasubramaniam, 2009).

Erosion Corrosion also results from the combined effect of the abrading action of vapours, gases and liquids and the mechanical rubbing action of solids over the surface of metals. This type of corrosion is caused by the breakdown of a protective film at the spot of abrasion. Abrading action removes protective films from localized spots on the metal surface, thereby resulting in the formation of differential cell at such areas and localized corrosion at anodic points of the cells. Erosion corrosion is most common in agitators, piping, condensers, tubes and vessels in which steams of liquids or gases emerge from an opening and strike the side walls with high velocities. Erosion corrosion is the deterioration of metals and alloys due to relative movement between surfaces and corrosive fluids. Depending on the rate of this movement, abrasion takes place. This type of corrosion is characterized by grooves and surface patterns having directionality. Typical examples are Stainless alloy pump impeller, Condenser tube walls, etc. (Barker *et al.,* 2011).

Inter-Granular Corrosion

Intergranular corrosion is the localized anodic dissolution of materials along grain boundaries. It occurs in a narrow region (typically 1-50 mm wide) in the vicinity of grain boundaries, which are completely corroded away so that the otherwise unattacked grains can fall apart. The grain boundary where the metal is sensitive undergoes corrosive attack (Mankowski and Szklarska-Smialowska, 1977). The grain boundary contains a material which shows more anoidic potential. The metal at the grain boundary decays as it becomes anodic and the centre of the grain becomes cathodic which is protected. It is mainly prevalent in stainless steels when heated to temperatures between 500 – 950°C for sufficiently long periods of time, thus permitting the formation of small sensitized precipitate particles of chromium carbide, $Cr_{23}C_6$, due to reaction between chromium and carbon in the steel . This occurs along grain boundaries leaving chromium-depleted zone adjacent the grain boundary susceptible to corrosion. (Mankowski and Szklarska-Smialowska, 1977)

Filiform Corrosion

Filiform corrosion only occurs if the surrounding atmosphere is humid enough for the salts depositing on filament heads to be dissolved. Even though the relationship between relative humidity and the corrosion rate can be influenced by the nature of the system concerned, a relative humidity value of 80-85% is widely accepted as optimal for filiform corrosion to develop (Sharma, 1944).

Filiform corrosion was first investigated by Sharman in 1944. It was described as a deterioration process that gives rise to corrosion products of a filamentous appearance under coatings. Filiform corrosion occurs in wet environments and usually arises from surface defects in the protective film in the presence of soluble ionic species. The attack usually affects steel,

aluminium and magnesium coated with an organic film (Sharman, 1994). Filifom corrosion usually starts at discontinuities, breaks, etc of the coating. Therefore, the phenomenon occurs most strongly at piece joints, where relative position changes are sufficient to produce small defects where corrosion will be maximal. Equally prone are aluminium profiles for exterior carpentry, which are coated with thin films that are therefore more liable to break. The more acute the angles, the thinner is the paint film and hence the higher the likelihood of filiform corrosion developing (Bautista, 1996).

Stress Corrosion Cracking

Stress corrosion is due to the combined effect of the static tensile stresses and the corrosive environment of the metal. The tensile stress is usually observed in fabricated articles like alloys of Zn and Ni. For stress corrosion cracking (S.C.C.) to occur it must fulfill these three requirements that there must be the presence of a tensile stress and this could be residual, locked in or applied stress; a material that is susceptible having a favorable microstructure; and an enabling environment such as a favorable temperature, pH, dissolved oxygen, chloride ion, carbon dioxide, hydrogen sulfide, etc. SCC may also initiate from pits and it occurs in different media (e.g. alkaline SCC also known as Caustic cracking). SCC could also be aggravated in the presence of chloride concentration and some other species. This form of corrosion is of limited occurrence with only aluminum alloys, in particular the higher strength materials such as the Al-Zn-Mg-Cu type and some of the Al-Mg wrought and cast alloys with higher magnesium content. The occurrence of stress corrosion increases in these alloys after specific low temperature heat treatments such as stove enameling (Kolawole *et al*., 2016).

Basic Definition of Corrosion

Ahmad (2006) defined corrosion as the destruction of structural materials under the chemical or electrochemical action of surrounding. Fontana, *et al*. (1979), in their study also defined corrosion as the reaction of metallic materials with its environment. They also defined corrosion as the degradation by reaction with its environment (oxygen, moisture, acid, and even alkalis) regardless of whether elastomer or ceramic. According to Roberts (2000) it could also be defined as the destructive attack of a metal in an environment by chemical or electrochemical process usually associated with a change in the oxidation state of a metal, oxide or semiconductor. Corrosion is the gradual deterioration of a metal by chemical or electrochemical reaction with the environment (Ahmad, 2006). Landolt (2007) defined corrosion as an irreversible interfacial reaction of a material with its environment. Corrosion is a thermodynamically feasible process because it is associated with negative changes of the Gibbs free energy (Singh and Quraishi, 2010).

1.1 Statement of Research Problem

A common difficulty faced in the material industry is a phenomenon well known as corrosion, and is commonly seen on iron ore as rust, this has led to various corrosion inhibition studies. Previous studies had shown that starch-silver nanoparticles exhibits promising corrosion inhibitory properties. However, the effect of starch-silver nanoparticles and honey on the corrosion behaviour of mild steel has not been explored in previous literature. The growth of fungi in the medium (inhibitors) undermines inhibition efficiency. Thus, the relative acidic pH of honey (3-3.5) helps to prevent the growth of fungi and bacteria, hence, the exploration of its possible synergistic effect to further improve inhibition efficiency.

1.2 Aim and Objectives

This research aims to study the effect of honey on synthesized starch-silver nanoparticles for the inhibition of mild steel corrosion in acid medium.

The aim will be accomplished by fulfilling the following research objectives:

1. Reduction of silver nitrate with soluble starch
2. Study the corrosion rate of mild steel in acid medium at different temperatures
3. Study the inhibition efficiency of starch-AgNPs on mild steel using weight loss method
4. Study the inhibition efficiency of honey as corrosion inhibitor
5. Evaluation of the synergistic effect of starch-AgNPs and honey
6. Elucidation of the absorption properties of starch-AgNPs and honey
7. Characterization of starch-silver nanoparticles (AgNPs).

1.3 Justification of Study

Synthesis of silver nanoparticles using green inhibitors such as starch is safe, cost effective and successful measure as mild steel corrosion inhibitors. Unlike the chemically synthesized inorganic inhibitors, greener inhibitors are safe and pose no health or explosive hazard in the laboratory. Recently, several studies have been carried out on the inhibition of the corrosion of mild steel. However, very few synergistic studies have been carried out on the corrosion inhibition of mild steel, as there are no literatures on the effect of honey on starch-silver nanoparticles for the corrosion inhibition of mild steel.

CHAPTER TWO

2.0 REVIEW OF RELATED LITERATURE

2.1 Nanotechnology

The terms *nanostructure*, *nanoscience*, and *nanotechnology* are currently quite popular in both the scientific and the general press. These intermediate-length structures are intriguing because generally in the nanometer region, almost all physical and chemical properties of systems become size-dependent. For example, although the color of a piece of gold remains golden as it reduces from inches to millimeters to microns, the color changes substantially in the regime of nanometers. Similarly, the melting points of such particles change as they enter the nanoscale, where the surface energies become comparable to the bulk energies. Because properties at the nanoscale are size-dependent, nanoscale science and engineering offer an entirely new design motif for developing advanced materials and their applications (Chelikowsky and Ratner, 2001).

Hughes (2000), presented the principles of AC electrokinetics for particle manipulation, reviewed the current state of AC electrokinetic techniques for the manipulation of particles on the nanometre scale, and considered how these principles may be applied to nanotechnology. The phenomena of dielectrophoresis and electrorotation, collectively referred to as AC electrokinetics, have been used for many years to study, manipulate and separate particles on the cellular (1 μm or more) scale. However, the technique has much to offer to the expanding field of nanotechnology, that is the precise manipulation of particles on the nanometre scale (Hughes, 2000).

According to Sweeny and Vaidyanthan (2003), rapid advances in nanoscience and nanotechnology are profoundly influencing the ways in which we conceptualiz the world of the future, and human ability to manipulate matter at the atomic and moleculs offers previously unimagined possibilities for scientific discovery and technological applications. The convergence of nanotechnology with biotechnology, information technology, cognitive science, and engineering may hold promise for the improvement of human performance at a number of levels.

Mnyusiwalla *et al.* (2003), in their report stated that, nanotechnology (NT) is a rapidly progressing field. Advances will have a tremendous impact on fields such as materials, electronics, and medicine. Nanoscience includes the study of objects and systems in which at least one dimension is 1-100 nm (Love *et al*., 2005). The objects studied in this range of sizes are larger than atoms and small molecules but smaller than the structures typically produced for use in microtechnologies (e.g., microelectronics, photonics, Micro-Electro-Mechanical Systems, and microfluidics) by fabrication methods such as photolithography. The dimensions of these systems are often equal to, or smaller than, the characteristic length scales that define the physical properties of materials. At these sizes, nano-systems can exhibit interesting and useful physical behaviors based on quantum phenomena (electron confinement, near-field optical effects, quantum entanglement, electron tunneling, and ballistic transport) or sub domain phenomena (superparamagnetism, overlapping double layers in fluids). Chemistry has played a key role in the development of nanoscience. Making and breaking bonds between atoms or groups of atoms is a fundamental component of chemistry; the products of those reactions are structures-molecules-that range in size from 0.1 to 10 nm (Love *et al*., 2005).

Nanotechnology is a multidisciplinary field, which covers a vast and diverse array of devices derived from engineering, biology, physics and chemistry. These devices include

nanovectors for the targeted delivery of anticancer drugs and imaging contrast agents. Nanowires and nanocantilever arrays are among the leading approaches under development for the early detection of precancerous and malignant lesions from biological fluids. These and other nanodevices can provide essential breakthroughs in the fight against cancer (Ferrari, 2005).

Adams and Barbante (2013) concluded that nanoscience has outgrown its infancy, and nanotechnology has found important applications in our daily life, with many more to come. Experimental advances since the 1980s and recognition of the potential of nanomaterials led to a genuine breakthrough of the inherently multidisciplinary nanoscience field. Analytical nanoscience and nanotechnology and especially the use of micro and nano eloctro mechanical systems, of these quantum dots and of mass spectrometry, currently provide one of the most promising avenues for developments in analytical science, derived from their two main fields of action, namely (a) the analysis of nano-structured materials and (b) their use as new tools for analysis.

Bajwa *et al*. (2013), reported that, nano originates from the Greek word meaning ‘‘dwarf’’. A nanometer is one billionth (10-9) of a meter, which is tiny, only the length of ten hydrogen atoms, or about one hundred thousandth of the width of a hair! Although scientists have used matter at the nanoscale for centuries, calling it physics or chemistry, it was not until a new generation of electron microscopes like scanning tunneling microscope (STM) and atomic force microscope (AFM) were invented in the 1980s that the world of atoms and molecules could be seen, manipulated and controlled.

2.2 Nanoparticles Used as Anticorrosion

A research by Shchukin *et al.* (2006), disclosed a novel approach for the preparation of corrosion inhibiting pigment and its use in self-healing anti-corrosion coatings in the form of a powder or a suspension in which nanoparticles (e.g. SiO_2, ZnO_2 TiO_2 nanoparticles) are coated layer-by-layer (LBL) with one or more layers of polymers or polyelectrolyte shell responsive to a specific stimulus or trigger. These particles thus act as nanoscale reservoirs for the effective storage of the corrosion inhibitors (e.g quinaldic acid and mercaptobenzotriazole). The method of producing the intelligent coating was reported to be cost effective and easy to implement, as the nano reservoirs provided prolonged release of the inhibitor. The corrosion inhibitors were released in a regulated fashion, mainly to the damaged coating zone and/or providing active, long term, corrosion protection of the coated substrate (e.g. steel and aluminum alloys).

Solomon and Umoren (2016), also studied the anticorrosion properties of polypropylene glycol/silver nanoparticles (PPG/AgNPs) using weight loss technique. Mild steel specimens in triplicates were suspended freely in glass reaction vessels containing 200 ml of test solutions (0.5 M H_2SO_4; 50, 100, 500, 750 and 1000 ppm PPG/AgNPs) at 303–333 K in a thermostated bath. The specimens were retrieved after 2 h progressively for 10 h, immersed in 1 M HCl for 1 min then washed under running water thoroughly with bristle brush, rinsed several times in distilled water, dried with warm air and then re-weighed. The average weight loss, in grams, was taken as the difference in the weight of the mild steel specimens before and after immersion in different test solutions.

In yet another study, Kolpak *et al*. (2007), bipolar pulsed current was used in the production of alloy deposits with a specified nanocrystalline element, the ore being most electro

active and at least one of which is a metal. For the electro deposition, an auxiliary electrode and the article to be treated (as the second electrode) are placed in the liquid comprising dissolved species of at least these two element and coupled to a power supply configured to supply electrical potential having periods of positive polarity and negative polarity at different times. The technology can be used to provide a substrate of electro conductive plastic or metal (e.g steel, aluminum and brass) with decorative or protective coatings featuring superior microscopic quality and/or resistance to corrosion and abrasion.

Saji and Thomas (2007), also shed light on the use of nanoparticles in treatment of surfaces and the method of providing such treatments for forming a beneficial oxide coating (e.g thin and non spalling oxide layers) on alloys, thereby providing the substrate with enhanced resistance to damaging oxidation and corrosion under extreme conditions. The invention in this category discloses a nano-crystal austenite steel bulk material with an improved corrosion resistance superior hardness and toughness, compressing an aggregate of austenite nano-crystal grains containing solid solution type nitrogen in an amount of 0.1 to 2.0% (Miura *et al.,* 2010).

Shi (2010), stated that nanotechnology has been playing an important role in supporting innovative technological advances to manage the corrosion of steel. In his research work on the use of nanotechnology to manage steel corrosion, nanoparticles were used in coating to prevent corrosion of steel in harsh environment (e.g sea water). Such nano-scale addition can be used at a much lower concentration (typically 2-5 wt %) than the conventional-grade fine pigment (typically 50-70 wt %) without the loss of corrosion resistance, thus providing the coating with much higher optical gloss and smoothness and reduce the risk of cracking. The electrochemical testing of coated mild steel substrates indicated the nano-scale additive impacted high corrosion resistance of the coating relative to the commercial grades. In one example, the coating

containing the nano-scale additive withstood a harsh chloride laden environment at 50^{o}C even for 3 hours, whereas the coating containing the commercial-grade additive failed immediately within 1 hour.

Homogeneous epoxy coatings containing nanoparticles of SiO_2, Zn, Fe_2O_3 and halloysite clay were successfully synthesized on steel substrate by room temperature curing of a fully mixed epoxy slurry diluted by acetone. The surface morphology and mechanical properties of these coating were characterized by scanning electron microscopy and atomic electron force microscopy, respectively. The effect of incorporating various nanoparticles on the corrosion resistance of epoxy-coated steel was investigated by potentiodynamic polarization and electrochemical impedance spectroscopy. The electrochemical monitoring of the coated steel over 28days of immersion in both 0.3 wt% and 3 wt% NaCl solutions suggested the beneficial role of nanoparticles in significantly improving the corrosion resistance of the coated steel, with the Fe_2O_3 and halloysile clay nanoparticles, found to significantly improve the microstructure of the coating matrix and thus enhance both the anticorrosive performance and Young's modules of the epoxy coating (Rathish *et al*., 2013).

2.3 Corrosion Inhibitors

Abdallah (2004), studied the corrosion behavior of aluminium in 2 cm^3 HCl solution in the presence and absence of four compounds of antibacterial drugs using hydrogen evolution, weight loss and potentiostatic polarization technique. It was found that the inhibition efficiency of these compounds depends on their concentration and chemical structure. The synergistic effect of halide ions on the corrosion inhibition of aluminium in H_2SO_4 using 2-acetylphenothiazine at temperature range of 30 – 60^{o}C was studied using the weight and

thermometric techniques. The decrease in inhibition efficiency and surface average was found to be in order I > Br > Cl which clearly indicates that the radii and the electronegativity of halides play a significant role in the absorption process.

A study by Acharya and Upadhyay (2004), was the first that reported impressive result on the corrosion inhibition of mild steel in 3.4% sodium chloride solution containing various concentrations of floxacin, amifloxacin, enofloxacin, pefloxacin and ciprofloxacin.

According to Oguzie *et al*. (2005), it has become a common practice to carry out quantum chemical calculation in corrosion studies. The study of corrosion processes and their inhibition by organic inhibitors is a very active field of research. Many researchers reported that the inhibition effect mainly depends on some physio-chemical and electronic properties of the organic inhibitor which relates to its functional group, steric effects, electronic density of donor atoms, orbital character of donating electrons, and so on. The inhibiting mechanism is generally explained by the formation of a physically and chemically absorbed film in the metal surface.

Oguzie *et al*. (2005), also studied the corrosion inhibition of aluminium and mild steel in H_2SO_4 in presence of methylene blue at 30 – 40 $^{\circ}$C using the weight loss technique. The result showed that the inhibition efficiency increased with increase in temperature within the range of 30 – 40 ^{o}C. The addition of halides (KCl, KBr and Kl) was found to enhance the inhibition efficiency. Since steel was discovered in 1913 by Harry Brearley in England (Cobb, 2010), it has become one of the most commonly used materials in daily life, being used for various kinds of industrial and engineering designs where they are deployed in various services, environments containing acids, alkalis and salt solutions. These service environments readily lead to inevitable corrosion of exposed surfaces of the metals because of their aggressive nature and best method to

protect these steels deployed in these corrosive environments is by the use of corrosive inhibitors (Oguzie *et al*., 2005).

It is well known that organic compounds which acts as inhibitors are rich in heteroatoms such as sulphur, nitrogen and oxygen. Pure metals and alloys react chemically/electrochemically with corrosive media to form stable compound in which the loss of metal occurs. The compound so formed is called corrosion product and the metal surface becomes corroded (Okafor *et. al.*, 2006).

Anticorrosion or corrosion inhibitors are in solid form. Most solids are relatively pure but sometimes a solid inhibitor is fused with another ingredient where a controlled rate of solubility is required. Liquids are usually preferred because of the ease with which they can be transported, measured and dispersed. Organic inhibitors seldom have optimum characteristics of viscosity, freezing or boiling point. Therefore, they are dissolved in an appropriate solvent to achieved desired properties. Corrosion inhibitors are usually compared on the basis of their inhibitor efficiency which is the percentage that corrosion is lowered in their presence as compared to the corrosion rate which occurs in their absence (Machnikova *et al.*, 2008).

Obot and Obi-Egbedi (2010) also shed light on inhibition effect of nizoral by distinguishing the type of metal (aluminium) and acid environment (HCl). An improved performance of ketoconazole was recorded in the case of ketoconazole with iodine mixture. Physisorption of this drug was suggested with regard to the calculated values of ΔG_{ads} -13.77 and -19.72 KJ/mol, for ketoconazole and ketoconazole with iodine mixture respectively. It is important to recognize, however, that in aqueous solutions, almost all the drugs are subject to some form of chemical degradation.

Mobin *et al.* (2011) studied the corrosion inhibition of mild steel in 0.1 M H_2SO_4 in presence of starch (polysaccharide) using weight loss and potentiodynamic polarization measurements in the temperature range of 30 – 60° C. Starch inhibits the corrosion rates of mild steel to a considerable extent; the maximum inhibition efficiency being 66.21% at 30^oC in presence of starch concentration of 200 ppm. In their study, the effect of the addition of very small concentration of sodium dodecyl sulfate and cetyl trimethyl ammonium bromide on the corrosion inhibition behavior of starch was also reported. The inhibition efficiency of starch significantly improved in presence of both the surfactants. The effect of surfactants on the corrosion inhibition behavior of starch appears to be synergistic in nature.

Paul and Machunda (2016), investigated the corrosion inhibition of *Aloe lateritia* gel for mild steel in 2 M HNO_3 and 1 M H_2SO_4 solutions by potentiodynamic polarization, Scanning Electron Microscopy (SEM) and Foutier transform infrared (FT-IR). They reported that the Inhibition efficiency increased with the increase of the concentration of the gel. The optimal concentration of the gel gives maximum inhibition efficiency of 77.4% and 70.3% in 1 M H_2SO_4 and 2 M HNO_3 respectively. Polarization plots show that, the gel works as a mixed type inhibitor altering both cathodic and anodic reaction.

2.4 Health and Environmental Impact of Nanoparticles

Colvin (2003), reported that Information about nanoparticle exposure conditions is only useful when paired with characterization of nanomaterial biological effects. This term refers broadly to data that can include experiments ranging from *in vitro* cellular toxicology to more traditional measurements of the lethal dose (LD50; statistically derived dose of a chemical/physical agent expected to kill 50% of organisms in a given population) of substances

in animals. Because of the relative lack of data on engineered nanoparticles, any treatment of this topic must necessarily rely on a patchwork of distantly related information from pulmonary particle toxicology to biomaterial compatibility studies. More specific information concerning nanoparticle clearance and bioavailability can be gleaned from studies aiming to develop nanomaterials for biotechnology.

Over the past decade, significant effort has been devoted to explore the use of nanoparticles in the fields of biology and medicine. Several different types of nanoparticles have successfully made their way into preclinical studies in animals, clinical trials in patients, and commercial products used in routine clinical practice. For example, gold nanoshells, quantum dots and super paramagnetic nanoparticles that carry target-specific ligands have been employed for *in vivo* imaging of cancerous cells, drug molecules have been packaged into polymer-based nanoparticles (Jiang *et al*., 2004).

Dreher (2004), in his study stated that the microtechnology of the second half of the 20th century has produced a technical revolution that has led to the production of computers and the Internet and taken us into a dynamic emerging era of nanotechnology. Nanomaterials are important due to their unique properties that may lead to new and existing applications. The current scenario of application is application of nanotechnology in the field of corrosion prevention of metals nano-sized particles may act differently in the environment. Perhaps becoming more easily dispersed than their counterparts, or just the opposite sinking into sediments or setting on soil making them more likely to be ingested by marine creatures able to strip chemicals from sediments and soil particles (Shankar *et al*., 2004).

Moore (2006), in a review, addressed the possible hazards associated with nano materials and harmful effects that may result from exposure of aquatic animals to nanoparticles. Possible nanoparticles association with naturally occurring colloids and particles was considered together with how this could affect their bioavailability and uptake into cells and organism. Uptakes by endocytotic routes were identified as probable major mechanism of entry into cells; potentially leading to various types of toxic cell injury. The higher level consequences for damage to animal health, ecological risk and possible food chain risks for humans are also considered based on known behaviours and toxicities for inhaled and ingested nanoparticles in the terrestrial environments.

Jeng and Swaanson (2006), assessed the toxicity profile of metal oxide nanoparticles proposed for use in industrial production methodology. Metal oxide nanoparticles used in this study included TiO_2, ZnO, Fe_3O_4, Al_2O_3, and CrO_3 with particle sizes ranging from 30 to 45 nm. Cellular morphology, mitochondrial function, membrane leakage of lactate dehydrogenase (LDH), permeability of plasma membrane, and apoptosis were assessed under controlled and exposed conditions (2 to 72 h of exposure). The microscopic studies demonstrated that nanoparticle-exposed Neuro-2A cells (especially ZnO) at doses >100 μg/mL became abnormal in size, displaying cellular shrinkage, and detachment from the surface of flasks. Mitochondrial function decreased significantly in the cells exposed to ZnO at 50 to 100 μg/mL. However, Fe_3O_4, Al_2O_3, and TiO_2 had no measurable effect on the cells until the concen/trations exceeded 200 μg/mL. LDH leakage significantly increased in the cells exposed to ZnO (50 to 100 μg/mL), while other nanoparticles tested displayed LDH leakage only at higher doses (>200 μg/mL). Flow cytometer tests showed that apoptosis took place in cells exposed to ZnO nanoparticles. More cells became necrotic as the concentrations increased.

The success of nanotechnology will require assurances that the products being developed are safe from an environmental, health, and safety (EHS) standpoint. In this regard, it has been previously reported in pulmonary toxicity studies that lung exposures to ultrafine or nanoparticles (particle size below 100 nm) produce enhanced adverse inflammatory responses when compared to larger particles of similar composition. Surface properties (particularly particle surface area) and free radical generation, resulting from the interactions of particles with cells may play important roles in nanoparticle toxicity. Health and environmental risk evaluations are products of hazard and exposure assessments (Warhiet, 2008).

Kumari *et al.* (2009), investigated cytotoxic and genotoxic impacts of silver nanoparticles using root tip cells of *Allium cepa* as an indicator organism. *A. cepa* root tip cells were treated with four different concentrations (25, 20, 75, and 100 ppm) of engineered silver nanoparticles (below 100 nm size) dispersion, to study endpoints like mitotic index, distribution of cells in mitotic phases, different types of chromosomal aberrations, disturbed metaphase, sticky chromosome, cell wall disintegration, and breaks. For each concentration five sets of microscopic observations were carried out. No chromosomal aberration was observed in the control (untreated onion root tips) and the mitotic index (MI) value was 60.3%. With increasing concentration of the nanoparticles decrease in the mitotic index was noticed (60.30% to 27.62%). The different cytological effects including the chromosomal aberrations were studied in detail for the treated cells as well as control. The findings also suggest that plants as an important component of the ecosystems needs to be included when evaluating the overall toxicological impact of the nanoparticles in the environment.

Although, mankind stands to obtain great benefits from nanotechnology, it is important to consider the potential health impacts of nanomaterials (NMs). This consideration has launched

the field of nanotoxicology, which is charged with assessing toxicological potential as well as promoting safe design and use of NMs. Although no human ailments have been ascribed to NMs thus far, early experimental studies indicate that NMs could initiate adverse biological responses that can lead to toxicological outcomes. One of the principal mechanisms is the generation of reactive oxygen species and oxidant injury. Because oxidant injury is also a major mechanism by which ambient ultrafine particles can induce adverse health effects, it is useful to consider the lessons learned from studying ambient particles (Xia *et al*., 2009).

According to El badawy *et al*. (2010), the extensive numbers of applications of silver nanoparticles (AgNPs), their potential impacts, once released into the environment, are of great concern. The toxicity of AgNPs was reported to be dependent on various factors such as particle size, shape and capping agent. These AgNPs were: uncoated H_2-AgNPs, citrate coated AgNPs (Citrate AgNPs), polyvinylpyrrolidone coated AgNPs (PVP-AgNPs), and branched polyethyleneimine coated AgNPs (BPEI-AgNPs).

Levard, *et al.* (2012), in their study reported that Silver nanoparticles (Ag-NPs) readily transform in the environment, which modifies their properties and alters their transport, fate, and toxicity. It is essential to consider such transformations when assessing the potential environmental impact of Ag-NPs. This review discusses the major transformation processes of Ag-NPs in various aqueous environments, particularly transformations of the metallic Ag cores caused by reactions with (in)organic ligands, and the effects of such transformations on physical and chemical stability and toxicity. Thermodynamic arguments are used to predict what forms of oxidized silver will predominate in various environmental scenarios. Silver binds strongly to sulfur (both organic and inorganic) in natural systems (fresh and sea waters) as well as in wastewater treatment plants, where most Ag-NPs are expected to be concentrated and then

released. Sulfidation of Ag-NPs results in a significant decrease in their toxicity due to the lower solubility of silver sulfide, potentially limiting their short-term environmental impact.

2.5 Preparation of Silver Nanoparticles

Shankar *et al.* (2004) in their study synthesized Ag–Au bimetallic nanoparticles. 90 cm^3 of a 1:1 0.001 M solution of $AgNO_3$ and $HAuCl_4$ was taken along with 10 cm^3 of Neem broth. The reduction of pure Ag^+ and Au^{3+} ions and that of the 1:1 $Ag+:AuCl^-_4$ mixture was monitored by measuring the UV–Vis spectra of the solution at regular intervals after diluting a small aliquot (0.2 cm^3) of the sample 20 times. UV–vis spectra were recorded as a function of time of reaction on a UV spectrophotometer operated at a resolution of 1 nm.

Solomon and Umoren (2016) prepared silver nanoparticles by mixing aqueous solutions of the polypropylene glycol (PPG) and $AgNO_3$ solution. The preparation was done in three phases. Firstly, different concentrations (50 ppm, 100 ppm, 500 ppm, 750 ppm, and 1000 ppm) of the polymer were prepared in 0.5 M H_2SO_4 solution. Secondly, the respective concentration of the polymer solution was used to prepare 1 mM $AgNO_3$ solution. Thirdly, to every 100 cm^3 of the respective mixture, 5 cm^3 of natural honey which served as reducing and capping agents was added.

Safaepour *et al*. (2009) in their research described that aqueous solution containing silver ion (1 mM) are prepared by adding 100µl of 1% w/v aqueous solution of polyethylene glycol 4000 mg to 90 cm^3 of silver nitrate solution. This was then alkalized with 0.1 M NaOH (20 µl) and treated in a microwave oven (850w) for 40 seconds for the reduction of metal ion. The reduction of Ag^+ ion by geraniol in the solution was monitored by sampling the aqueous component (2ml) and measuring the UV-Visible spectrum of the solutions. Furthermore, the

silver nanoparticles where characterized by Transmission Electron Microscopy (TEM) and Energy Dispersive Spectroscopy (EDS).

Safaepour *et al*. (2009) reported the chemical reduction of an aqueous solution of silver nitrate as one of the most widely used method for synthesizing silver nanoparticles. In their studies, they reported that the colour change from colourless to geranial brown in the reaction vessel, suggested the formation of AgNps. They characterized the AgNPs by UV Visible spectroscopy operated at a resolution of 2 nm from 100-1000 nm and observed a strong, broad absorption band with a maximum located at 440 nm.

Geethalakshmi and Sarada (2010) carried out a research on synthesis of plant-mediated silver nanoparticles using *Trianthema decandra* extract. 1 mM aqueous solution of silver nitrate ($AgNO_3$) was prepared and used for the synthesis of silver nanoparticles. 10 cm^3 of *Trianthema decandra* root extract was added into 90ml of aqueous solution of 1 mM silver nitrate for reduction into Ag^+ ion and kept at room temperature for 5hours.

Prasad *et al*. (2011) in their research paper "Biogenic Synthesis of Silver Nanoparticles using *Nicotiana tobaccum* leaf extract and study of their antibacterial effect", explained the preparation of silver nanoparticles from tobacco leaf extract. They explained that in a typical synthesis of silver nanoparticles, requisite amount of $AgNO_3$, 1 mM for 50 cm^3 was added to 48 cm^3 of deionized milli-Q water. The leaf extract (2 cm^3) was added drop wise into the solution of $AgNO_3$. The content was later on placed onto a rotary orbital shakar operating at 200 rpm for 48hours. The incubation of the mixture was carried out at 30^oC in dark condition. The reduction of silver ion was monitored by sampling an aliquot (3 cm^3) of the mixture at intervals of 24 hours, followed by measurement of the UV-Vis spectra using a spectrophotometer. A spectral

scanning analysis was carried out by measuring optical density of the content from wavelength, 300 to 700 nm in order to find the highest peak or λmax.

Patil *et al*. (2012) reported the synthesis of silver nanoparticles using *Ocimum tenuiflorum* leaf extract as reducing and stabilizing agent. An aqueous solution of silver nitrate (1 x 10^{-3} M, 20 cm^3) was added to 2 cm^3 of *Ocimum tenuifiorum* leaves extract. After 10 minutes the solution turns yellow to yellow red to dark brown indicating the formation of AgNps. They also reported UV-Visible characterization using UV-Visible spectrophotometer and observed an intense Surface Plasmon Resonance (SPR) band at maximum wavelength of 450 nm revealing the formation of AgNps.

Tran-Quang *et al.* (2013) synthesized silver nanoparticles by using 1.7 g (1.0 x 10^{-2} mol) of silver nitrate. The sample was dissolved in 100 cm^3 of deionized water and precipitated using 0.62 g (1.55 x 10^{-2} mol) of sodium hydroxide. Their process of silver nanoparticles preparation under UV treatment was controlled by the irradiation time. The period was found to be optimal for the complete reduction of silver varied from 8.9 nm to 12 nm with the increase of silver concentration. It was obvious that with an increase in concentration, the colour of solution turned from colourless to light yellow then dark yellow and then brown. He emphasized that the changes in colour suggest the formation of silver nanoparticles in the solution and the absorption band of colloidal solution of the synthesized silver nanoparticles was observed at the 422 nm using a spectrophotometer.

Kumar *et al.* (2014) in their research evaluated the synthesis of novel and stable N-doped ZnO/g-C_3N_4 core–shell nanoplates with excellent visible-light responsive photocatalysis. Bulk g-C_3N_4 was prepared by directly heating melamine to 550 ^oC for 2 hours in N^2 atmosphere. Pure g-

C_3N_4 nanosheet was prepared by liquid phase exfoliation. In brief, 0.05 g of g-C_3N_4 was ultrasonicated in 50 cm^3 of water for 1 h and centrifuged to remove the unexfoliated g-C_3N_4. The ZnO nanoplates were prepared by using a co-precipitation method. 0.1 M metal precursor solution was directly mixed with 0.1 M aqueous solution of ammonium oxalate while stirring and kept for 1 hour at room temperature. The solution became cloudy and a white precipitate of zinc oxalate was obtained. The oxalate precursor was centrifuged, washed (thrice) with water and ethanol and dried at 80^oC for 1 hour.

Sadeghi (2014) analyzed the synthesis from 1 mM $AgNO_3$ solution using leaf extract at various concentrations as a reducing and capping agent. The silver nanoparticles exhibit yellow-dark yellowish brown colour in aqueous solution. UV-Vis spectral analysis was done by using UV-Vis spectrometer and recorded as a function of time. Absorption spectrum of AgNps formed in the reaction media at 10 minutes had an absorbance peak at 430 nm, broadening of peaks indicates that the particles are polydispersed.

Raghavendra *et al.* (2016) reported a step reduced synthesis of starch-silver nanoparticles. Silver nanoparticles were directly synthesized in a single step by microwave irradiation of a mixture of starch, silver nitrate, and deionized water. This is different from the commonly adopted procedure for starch-silver nanoparticle synthesis in which silver nanoparticles are synthesized by preparing a starch solution as a reaction medium first. Thus, the additional step associated with the preparation of the starch solution was eliminated. In addition, no additional reducing agent was utilized. In their report, starch acted as reducing agent. The obtained nanoparticles were spherical in shape with diameter 5 – 10 nm. It was also reported that starch influenced the sized of nanoparticles and the synthesized nanoparticles exhibited good antibacterial properties.

Lakshmanan *et al*. (2018) prepared silver nanoparticles using *Cleome viscosa* leaf extract. They used 3 mM solution of $AgNO_3$. They reported that 5 cm^3 of plant extract was mixed with 25 cm^3 of 3 mM $AgNO_3$. The solution changed from colourless to reddish brown indicating the formation of Ag nanoparticles. They also reported UV-Vis spectra analysis using a spectrophotometer at a resolution of 1 nm from 200 to 510 nm and observed maximum absorbance at the wavelength of 455 nm.

2.6 Characterization of Silver Nanoparticles (AgNP)

The size and shape of metal nanoparticles are typically measured by analytical techniques such as Transmission Election Microscopy (TEM), Scanning Electron Microscopy (SEM) or Atomic Force Microscopy (AFM) (He *et al*., 2004). Measuring the aggregation state of the particle requires a technique to measure the effective size of the particles in solution such as Dynamic Light Scattering (DLS) or analytical disc centrifugation (Sosa *et al.*, 2003). However, due to the unique optical properties of silver nanoparticles, a great deal of information about the physical state of nanoparticles can be obtained by analyzing the spectra properties of silver nanoparticles in solution (Sun *et al*., 2000). Other variety of technique includes X-ray photoelectron spectroscopy (XPS), powder X-ray diffractometry (XRD), Fourier transform infrared spectroscopy (FTIR), and UV – Vis spectroscopy (Khomutov and Gubin, 2002). These techniques are used for determination of different parameters such as particles size, shape, crystalinity, fractal dimentions, pore size and surface area. Moreover, orientation, interrelation and dispersion of nanoparticles and nanotubes in nanocomposite materials could be determined by these techniques (Chimentao *et al*., 2004).

Shrivastava *et al.* (2007), studied to verify reduction of silver ions, the solution was scanned in the range of 200–600 nm in a spectrophotometer using a quartz cuvette with water as the reference. The size and morphology of the nanoparticles were analysed with a Transmission Electron Microscope. The sample was prepared by placing a drop of silver nanoparticles on carbon-coated copper grid and subsequently drying in air, before transferring it to the microscope operated at an accelerated voltage of 120 kV. The stability of the nanoparticles was examined by exposing them to ambient conditions for four weeks, followed by centrifugation at 15 000g for 15 min at RT to rule out formation of precipitate with time. The colour and pH of the solution were also checked at regular intervals, which hardly showed any change.

Gurunathan *et al*. (2009), in their report, synthesized silver nanoparticles and purified it by using sucrose density gradient centrifugation. The purified sample was further characterized by using UV-Vis spectra, fluorescence spectroscopy and TEM. The purified solution yielded maximum absorbance peak at 420 nm and the TEM characterization showed a uniform distribution of nanoparticles, with an average size of 50 nm. Xray diffraction (XRD) exihibits 2θ values corresponding to the silver nanocrystal. The size distribution of the nanoparticles ware determined using a particle-size analyzer and the average particle size was found to be 50 nm.

Zhou *et al*. (2011), in their study outlined a new detection strategy, based on the Faradaic charge transfer when AgNPs strike an electrode. Therein, they showed for the first time that the direct electro-oxidation of AgNPs colliding with an electrode is both viable and quantitative, and can be used for characterization and NP identification. First, a AgNP-modified GC electrode was scanned anodically in the citrate solution to observe the stripping voltammogram. Next, the GC microelectrode was placed in the citrate solution and dispersed AgNPs (diameter 20–50 nm) were added. Under potentiostatted conditions (from 50–500 mV vs. Ag/AgCl), oxidative

(Faradaic) current spikes were observed, showing for the first time that direct oxidation of metal NPs during collision events is both observable and quantitative.

Singh *et al.* (2013), reported the characterization of AgNPs as follows; after 168 hours of synthesis, the sample of AgNPs was centrifuged at 14,000 rpm for 30 minutes at room temperature. Repeated rinses were performed to remove impurities. The pellet of AgNPs was suspended in 1 cm^3 sterile Milli-Q water. The X-ray diffraction (XRD) data of dried thin films of AgNPs on a glass slide was recorded by D8 Advanced Brucker X-ray diffractometer with a Cu Kα (1.5Å) source. A drop of AgNP sample was dried on a glass slide for analysis under a Scanning Electron Microscope (SEM) at 20 kV accelerating voltage. Samples for Transmission Electron Microscopy (TEM) and high-resolution TEM (HR-TEM) were prepared by drop-coating the AgNPs solution on a carbon-coated copper grid and drying under infrared radiation. The presence of elemental silver was confirmed through Energy-Dispersive Spectroscopy (EDS). The particle size of a 3 cm^3 sample was estimated using a dynamic light scattering instrument in a polystyrene cuvette.

Cheng and Compton (2014), reported the direct detection and characterization of NPs via reduction and oxidation. The Compton group pioneered the new area of NP coulometry based on direct electrochemistry (such as oxidation and reduction) of individual NPs impacting at a solid ultramicroelectrode (UME). The advantages of NP coulometry are that it can derive a variety of information on the impacting NPs (e.g., the oxidative charge associated with an individual spike can be used to measure the size of an individual metal NP, such as silver, gold, nickel NPs, as reported previously). In a typical experiment to size NPs [e.g., nickel NPs (NiNPs)], a carbon-fiber microelectrode was placed in a degassed solution of 10 mM HClO4 and 100 mM NaClO4, and a known concentration of pre-dispersed NiNPs added. The electrode potential was held at

+1.7 V (relative to Ag/AgCl) for chronoamperometry and oxidative current spikes were observed, whilst no oxidative spikes were observed at 1.0 V, confirming that the current spikes corresponded to Faradaic oxidation of NiNPs [Ni(NP) - $2e^-$ Ni^2 + (aq)]. A relationship between diameter and charge of single NiNPs was established, based on assuming that NiNPs are spherical (diameter, Dnp) and that charge Q passed as a result of complete reduction of single NiNPs:

2.7 Application of Silver Nanoparticles (AgNP)

Silver nanoparticles are used to efficiently harvest light and for enhanced optical spectroscopies including Metal Enhanced Fluorescence (MEF) and Surface – Enhanced Raman Scattering (SERS). The synthesis of nanoparticles, however, is a fairly established field as particles of submicron or nanosized dimensions have been synthesized for centuries. The first example of considerable recognition is the Roman Lycurgus Cup, a bronze cup lined with colored glass that dates to the fourth Century AD. The glass scatters a dull green light and transmits red light. According to a study commissioned by the British Museum, who currently displays the cup, the glass contains 70 nm particles that are an alloy of silver (70%) and gold (30%) (Barber and Freestone, 1990).

Over the last decades silver nanoparticles have found application in catalysis, optics, electronics and other areas due to their unique size-dependent optical, electrical and magnetic properties. Currently, most of the applications of silver nanoparticles are in antibacterial/antifungi agent in biotechnology and bioengineering, textile engineering, water treatment and silver based consumer products. There is also an effort to incorporate silver

nanoparticles into a wide range of medical devices, including but not limited to bone cement, surgical instrument, surgical masks, wound dressings (Haynes and Duyne, 2001).

Fuller *et al*. (2002), reported that silver nanoparticles are used in conductive inks and integrated into composites to enhance thermal and electrical conductivity. Commercial silver pastes and inks generally provide thin-film conductivity up to only 2000 S cm-1, even with annealing temperatures >200 °C. Recently, conductive elements have been generated from silver nanoparticles, albeit at high annealing temperatures (>300 °C). Since the melting points of metal particles drop drastically in the extreme nanometer regime (<10 nm), it would thus be possible to significantly lower the annealing temperature of silver nanoparticles by reducing their particle size. However, the preparation of stabilized silver nanoparticles in the sub-10 nm range necessary to enable low-temperature coalescence to conductive elements remains a synthetic challenge (Li *et al*., 2005). Silver nanoparticles of this size are known to scatter green light and transmit orange, and the addition of Au shifts the absorption band to longer wavelengths (Evanoff and Chumanov, 2005).

Samsung has created and marketed a material called silver nano that includes silver nanoparticles on the surface of household appliances (Jang *et al.,* 2006). Silver nanoparticles has been used as the cathode in a silver-oxide battery (Fisher, 2006).

Mohan *et al*. (2007), in their study, demonstrated that the hydrogel hybrid with different sizes of silver nanoparticles can be effectively employed as antibacterial material, because of the outstanding applications of the gel nanoparticle hybrids in various fields including biomedical applications. The concept of the present hydrogel network carrier approach was schematically presented. This approach was useful to precisely produce Ag nanoparticles. Another main

advantage of this methodology is that it provided uniformly distributed Ag nanoparticles within the networks and the formed hydrogel Ag networks can be effectively used for antibacterial applications. Silver nanoparticles are used in biosensors and numerous assays where the silver nanoparticles materials can be used as biological tags for quantitative detection (Mohan *et al*., 2007).

He *et al*. (2013) in their research, reported on the application of silver nanoparticles in clinical ultrasound gel. Based on the bactericidal activity of the AgNP, a clinical bactericidal ultrasound gel containing 10 μg/mL was developed with a longer duration, compared with that of 5 μg/mL. A total of 50 specimens used commercial ultrasound gel and 50 specimens used self-prepared AgNP ultrasound gel. The results indicated that bacterial contamination with *S. aureus* (ATCC 6538), *E. coli.* (ATCC 8099), *Pseudomonas aeruginosa*. (ATCC 15442), and *Candida albicans* (ATCC 10231) were found in all specimens using commercial gel, and no bacterial contamination was found from specimens using the self-prepared AgNP gel. Meanwhile, the image quality of ultrasound was evaluated in the preliminary trial, and the results demonstrated that there was no difference in the image quality between commercial gel and the self-prepared AgNP gel. Also, there were not any noncompliance and adverse effects observed both during and after the experiments.

Koseogulo *et al*. (2013) reported the use of silver nanoparticles in the preparation of polysulfone (PS) membranes by adding different amounts of silver nanoparticleAgNP (0–1 wt%) into the dope solution. The bare PS and AgNP entrapped PS membranes (AgNP-PS composite membrane) were tested for physical properties with water permeability, MWCO (molecular weight cut-off), AFM, contact angle and SEM analyses, filtration performances by using the model protein (BSA) and carbohydrate (dextran) solutions and biofouling resistances by using

real activated sludge. AgNP addition improved the protein and carbohydrate filtration performances of bare PS membrane. The results of biofouling experiments showed the AgNP-PS composite membranes having lower absorptive and pore fouling values than bare PS membrane. The ionic silver loss from membrane during pure water filtration was measured using inductive-coupled plasma spectrometer (ICP) and the results showed the minimum silver loss from the composite membranes. The results of disk diffusion test showed that the composite AgNP-PS membranes decreased the growth of bacterial colonies

Wei *et al*. (2015), reported that silver nanoparticles are employed in newly emerging applications as photosensitizers/radiosensitizers, antiviral and anticancer agents. Treatment of varieties of cancer with silver nanoparticles has been well documented. Silver nanoparticles (AgNPs) have been widely used in biomedical fields because of their intrinsic therapeutic properties such as: treatment of leukemia, breast cancer, hepatocellular carcinoma, and skin and/or oral carcinoma.

CHAPTER THREE

3.0 MATERIALS AND METHOD

3.1 Materials/Apparatus

All glasswares were washed thoroughly with detergent afterwards it was rinsed with distilled water. The materials used to carry out the study are as follows:

Volumetric flask

Beaker

Stirrer

Measuring cylinder

Weighing balance

Erlenmeyer flask

Funnel

Spatula

Mild steel coupon

Desiccators

3.1.1 Equipments

The equipments used for the study are as follows:

Hot plate, (Suart EW-04801-01)

Thermostatic water bath (Nikel Electro Clifton, NE1-14)

Centrifuge (Eppendorf, 5702 R)

Metal Analyzer (Scientific Niton, XL2 XRF, Germany)

UV-Visible spectrophotometer (Agilent, CARY 630)

Fourier Transformed Infared Spectrophotometer (Agilent, CARY 630).

3.1.2 Reagents

The following reagents were used for the study:

Silver Nitrate ($AgNO_3$)

Hydrochloric Acid (HCl)

Ethanol

Acetone

Starch

Honey

3.2.0 Materials

Silver nitrate, HCl, acetone and pure starch were purchased from Sigma Aldrich. The sheet of mild steel was obtained from Mechanical Engineering Department, Ahmadu Bello University Zaria.

3.2.1 Preparation of the Mild Steel

The mild steel sample obtained from Mechanical Engineering Department, Ahmadu Bello University Zaria was cut into coupons of length 49 mm and diameter 10 mm then it was sand papered to aid a thorough polishing so as to obtain a shinny surface. The mild steel was degreased with ethanol and dried with acetone (ASTM G1-90, 2011). The composition of the coupons were determined as follows Fe (99.25%), Mn (0.645%), C (0.12%) and Si (0.10%), this was estimated using Thermo Scientific Niton Metal Analyzer. All prepared steel samples were preserved in a desiccator. The analyzed samples were used for corrosion inhibition studies (Mobin, 2011).

3.2.2 Reagent Preparation

Appendix 1 shows a procedural preparation of the acid solution of 0.5 M HCl with a percentage purity of 36% and a specific gravity of 1.18, prepared in 250 cm^3 volumetric flask using deionized water. Similarly, an aqueous solution of 0.1 M $AgNO_3$ was prepared using deionized water in a 250 cm^3 volumetric flask (Obot *et al*., 2013).

3.2.3 Preparation of Standards

The starch solution was prepared by adding 500 mg of starch into a 1000 cm^3 volumetric flask, was shaken, and then made up to mark with boiling distilled water. It was allowed to boil for 1 minute then cooled at room temperature. Working concentrations of starch solutions were prepared and used for the study. These were prepared by diluting the stock solution in distilled water to give working concentrations as follows:

To prepare 500 cm^3 of the working solutions 1, 5, 10, 50, 100, and 200 cm^3 of the stock solution were respectively dispensed into a 500 cm^3 volumetric flask and made up to mark with boiling distilled water to give working concentrations (1, 5, 10, 50, 100, and 200 (mg/l)) respectively. The stock solution was also used as one of the working concentrations to give a total of seven (7) working solutions (Fanta *et al*., 2002).

Test for Bulk Density: The bulk density in g/cm^3 which is the weight per unit volume of the starch was ascertained by taking the weight of the starch and dividing it by the volume. This was done using the "measurement in a graduated cylinder method" (Kalra *et al*., 1995).

A quantity of the starch powder sufficient to complete the test was passed through a sieve with an aperture of 1.0 mm (to break up agglomerates that may have formed during storage). 100 g of

the test sample (m) was gently introduced into a dry graduated cylinder (250 cm^3), without compacting. The apparent volume (v) was read to the nearest graduated unit. The bulk density was calculated in g/cm^3 using the formula d = m/v, where, m=mass and v=volume (Kalra *et al*., 1995).

Test for pH: A pH meter was used to probe the hydrogen ion activity of the stock solution of starch, which was preceded by a litmus test. A sample solution was poured into a beaker, a piece of red and blue litmus paper was dipped into the solution to test for its alkalinity and acidity respectively. The absence of colour change in the litmus paper indicated neutrality (Kalra *et al.*, 1995). Standard buffer solution: one buffer tablet each of pH 4.0 and 7.0 was dissolved in distilled water separately and made up to 100 cm^3. Exactly 10 g of the air-dried and sieved (0.125 mm) starch powder was weighed into a glass container and 10 cm^3 of distilled water was added. The mixture was allowed to stand for 1 hour. The pH meter was turned on and allowed to warm for 15 minutes. The glass electrode was standardized using a standard buffer of pH 7.0 and thereafter, calibrated with the buffer pH = 4. The glass electrode of the pH meter was immersed in the mixture and the pH value to the nearest 0.1 unit was taken (Kalra, 1995).

3.3 Preparation of the Composite

The prepared 0.1 M aqueous solution of $AgNO_3$ was used for the synthesis of starch-silver nanoparticles. The respective concentrations of the working starch solutions were used to prepare the starch-AgNPs. The previously prepared aqueous solution of 0.1 M $AgNO_3$ was added to the respective starch solutions in two separate 250 cm^3 Erlenmeyer flask. The mixtures were thoroughly mixed by manual shaking and exposed to sunlight for 15 minutes (Obot *et al*., 2013). Natural honey (5 cm^3) was then added to one of the flasks (Solomon and Umoren, 2016). The

flask containing the honey was gently shaken and allowed to sit for 3 minutes. These were then used to carry out the corrosion study.

3.4.0 Characterization of Silver Nanoparticles (AgNP)

3.4.1 UV-Visible Spectroscopy

The bio reduced sample was confirmed by UV-Visible analysis. The obtained AgNPs were purified through repeated centrifugation for 20 minutes and washed with distilled water. The sample was analyzed by preparing dilute solution made in deionized water. The reduction of Ag ions was monitored from 300 – 800 nm with deionized water serving as blank (Yakout and Mostafa, 2015).

3.4.2 Fourier Transform Infrared Spectroscopy (FTIR)

The starch-AgNPs composite was obtained by evaporating to dryness the colloidal solution of the polymer nanoparticles in an oven using a petridish at 50°C (Solomon and Umoren, 2016). After which Fourier transformed infrared (FTIR) spectra of the nanoparticles were recorded.

3.4.3 Scanning Electron Microscopy (SEM)

The morphology of the composite nanoparticles samples were studied using a standard Agilent 360 Technology to study the pores and texture of the composite at varied magnifications (50 µm, 80 µm, 100 µm, and 200 µm).

3.5.0 Weight Loss Measurement

The weight loss experiment was performed for a duration of 8 hours (ASTM Committee G1–90, 2011). The pre-weighed and cleaned mild steel coupons were suspended with the aid of hooks in two separate 200 cm^3 beakers containing 0.5 M HCl (100 cm^3) and the content of the prepared starch-AgNPs respectively maintained at 30^oC in a thermostatic water bath. This process was repeated for 40^oC, 50^oC, 60^oC and 70^oC using freshly prepared starch-AgNPs each time. The mild steel coupons were weighed before and after the corrosion test with their respective weights recorded. The measurements were also carried out for an uninhibited solution to serve as control, a solution containing honey alone and another solution containing the combination of starch-AgNPs with honey (Mobin *et al.*, 2011; Solomon and Umoren, 2016).

The corrosion rates were determined using the equation: (James *et al.*, 2007)

$$\text{Corrosion rate (mpy)} = \frac{534W}{pAt} \qquad (1)$$

Where: 534 is a constant for the rate of corrosion in mils per year, W is weight loss in mg; p is the density of specimen in g/cm^3; A is the area of specimen in sq. inch and t is exposure time in hours.

The inhibition efficiency of the test solutions were evaluated using the following equation:

$$\text{inhibition efficiency (\%IE)} = \frac{\text{CRo} - CRi}{CRo} X\ 100 \qquad (2)$$

Where: CR_o is the corrosion rate of mild steel in absence of inhibitor and CRi is corrosion rate of mild steel in presence of inhibitor (James *et al.*, 2007)

3.5.1 Synergism Evaluation

The synergistic effect of the various concentrations of starch-AgNPs with honey for mild steel in 0.5 M HCl at different temperatures was considered.

The synergism parameters $S_{1,}$ was evaluated using the relationship:

$$S_1 = \frac{1 - I(1+2)}{1 - I'(1+2)}$$

Where, I(1+2) = (I_1 + I_2); I_1 is inhibition efficiency of starch-AgNPs and I_2 is inhibition efficiency of honey, and I'(1+2) = I'_{1+2} is inhibition efficiency of starch-AgNPs in combination with honey (Mobin *et al.*, 2011).

The values of the synergism parameters for the various concentrations of starch studied were calculated from the gravimetric data at 30^{o}C, 40^{o}C, 50^{o}C, 60^{o}C and 70^{o}C (Mobin *et al.*, 2011).

3.5.2 Adsorption Consideration

The character of adsorption of starch-AgNPs alone and starch-AgNPs in combination with honey was elucidated from the values of degree of surface coverage (θ) calculated from the weight loss data.

The plot of C/θ against C was drawn which is characteristics of Langmuir adsorption isotherm given by equation:

$$\frac{C}{\theta} = \frac{1}{k} + C$$

Where; θ is degree of surface coverage, k is the equilibrium constant of the adsorption process and C is the starch concentration.

CHAPTER FOUR

4.0 RESULTS

4.1 Synthesis of Starch-Silver Nanoparticles

The initial colourless solution turned brownish after irradiation for 15 minutes, which indicated that the nanoparticles was successfully synthesized (Shankar *et al*., 2004). A visible representation of the characteristic brown colouration can be seen in plate I and II.

4.2 Weight Loss Study

The result of corrosion study using mild steel as sample in 0.5 M HCl in the presence and absence of the inhibitor (starch-AgNPs) using weight loss technique at temperature range (30^oC, 40^oC, 50^oC, 60^oC and 70^oC) was studied and the plot of the inhibition efficiency against starch-silver nanoparticles concentration is shown in figure 4.1.

4.3 Sample Representation of Biosynthesized Composite

Plate I: Sample representation of biosynthesized composite of AgNPs using starch (1 mg/l)

Plate II: Sample representation of biosynthesized composite of AgNPs using starch (200 mg/l)

4.4.0 CHARACTERIZATION

4.4.1 UV-Visible Spectra

UV-Visible spectroscopy is one of the most widely used techniques for the structural characterization of silver nanoparticles (Venu, 2011). Figure 4.1 reveals the adsorption peak of starch-silver nanoparticles.

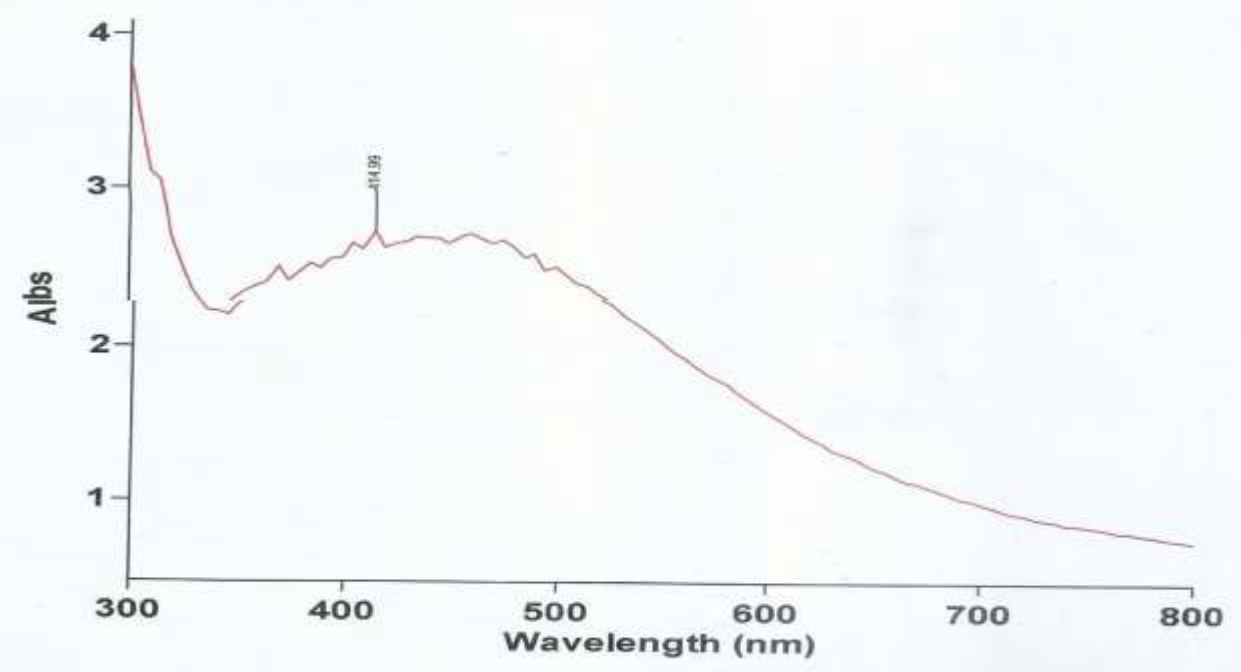

Figure 4.1: UV-Vis Spectrum of Starch-AgNPs

4.4.2 Fourier Transform Infrared Spectroscopy (FTIR)

The inhibitor Starch-AgNPs was subjected to FTIR for the determination of the functional groups' interaction of starch with the synthesized silver nanoparticles. Figure 4.2 and 4.3 shows the FTIR spectra of starch and starch-silver nanoparticles respectively.

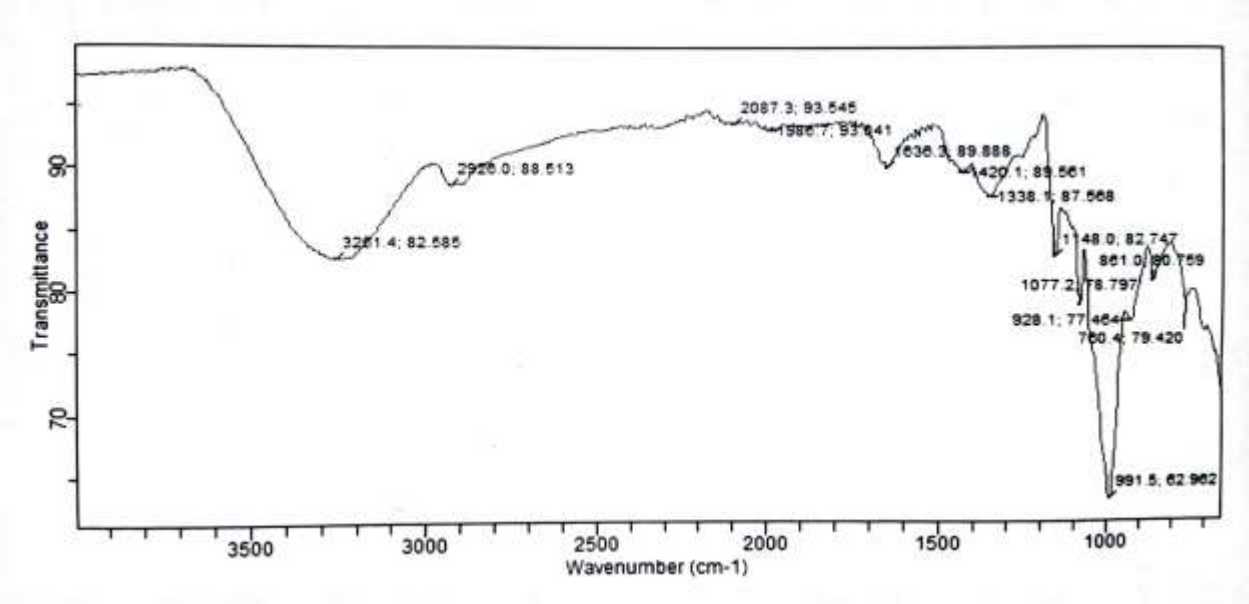

Figure 4.2: FTIR Spectrum of Starch

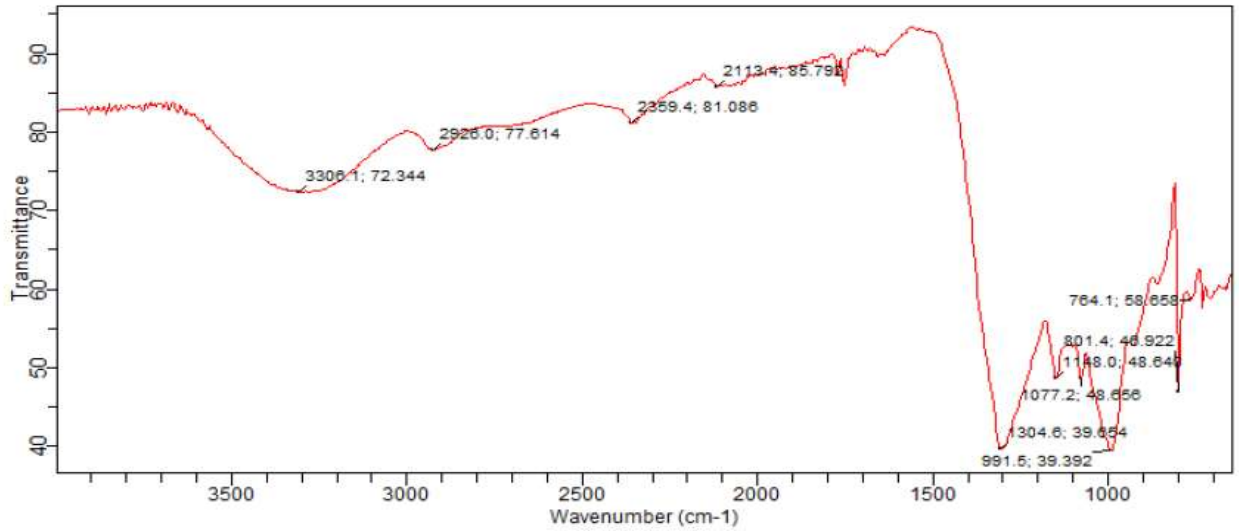

Figure 4.3: FTIR Spectrum of Starch-AgNPs

4.4.3 SEM Micrograph of Starch-Silver Nanoparticles

The morphology of starch-silver nanoparticles at different magnifications is represented in Plate III, IV, V and VI.

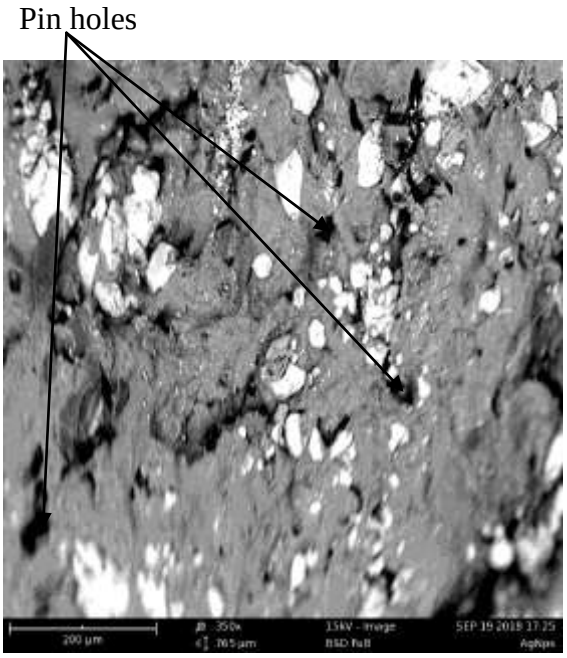

Plate III SEM micrograph at 200 µm

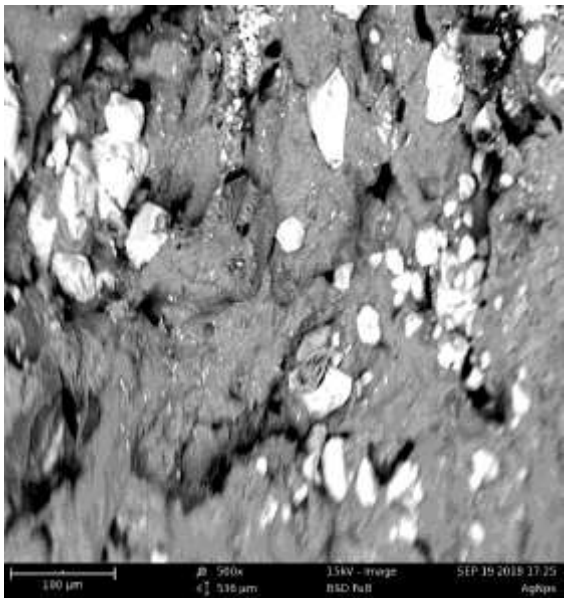

Plate IV SEM Micrograph at 100 µm

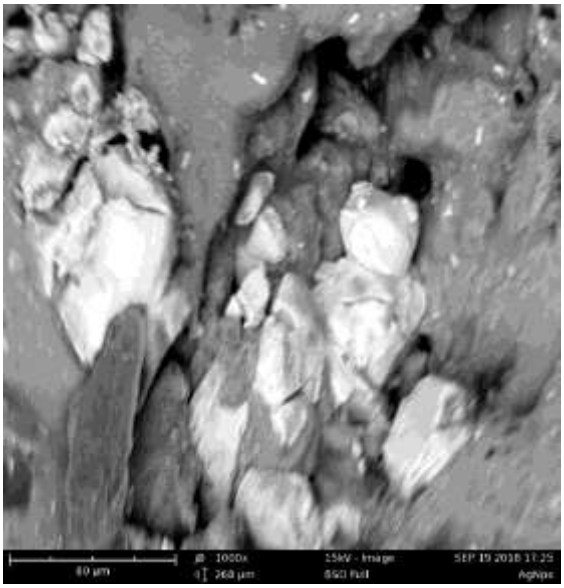

Plate V SEM Micrograph at 80 µm

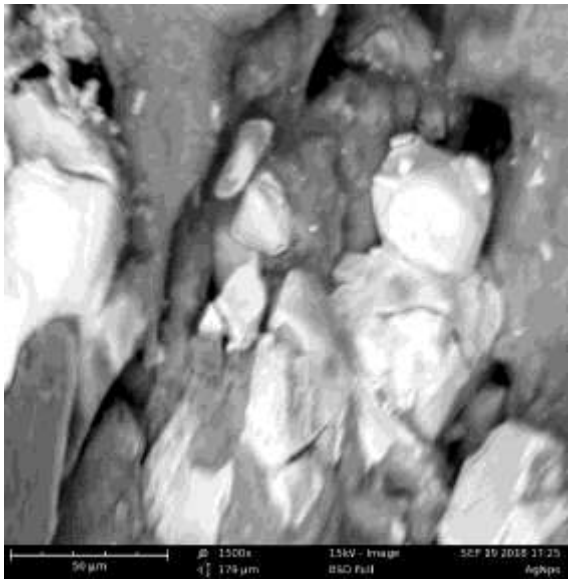

Plate VI SEM Micrograph at 50 µm

4.4.4 Mechanism of Starch-Silver Nanoparticles

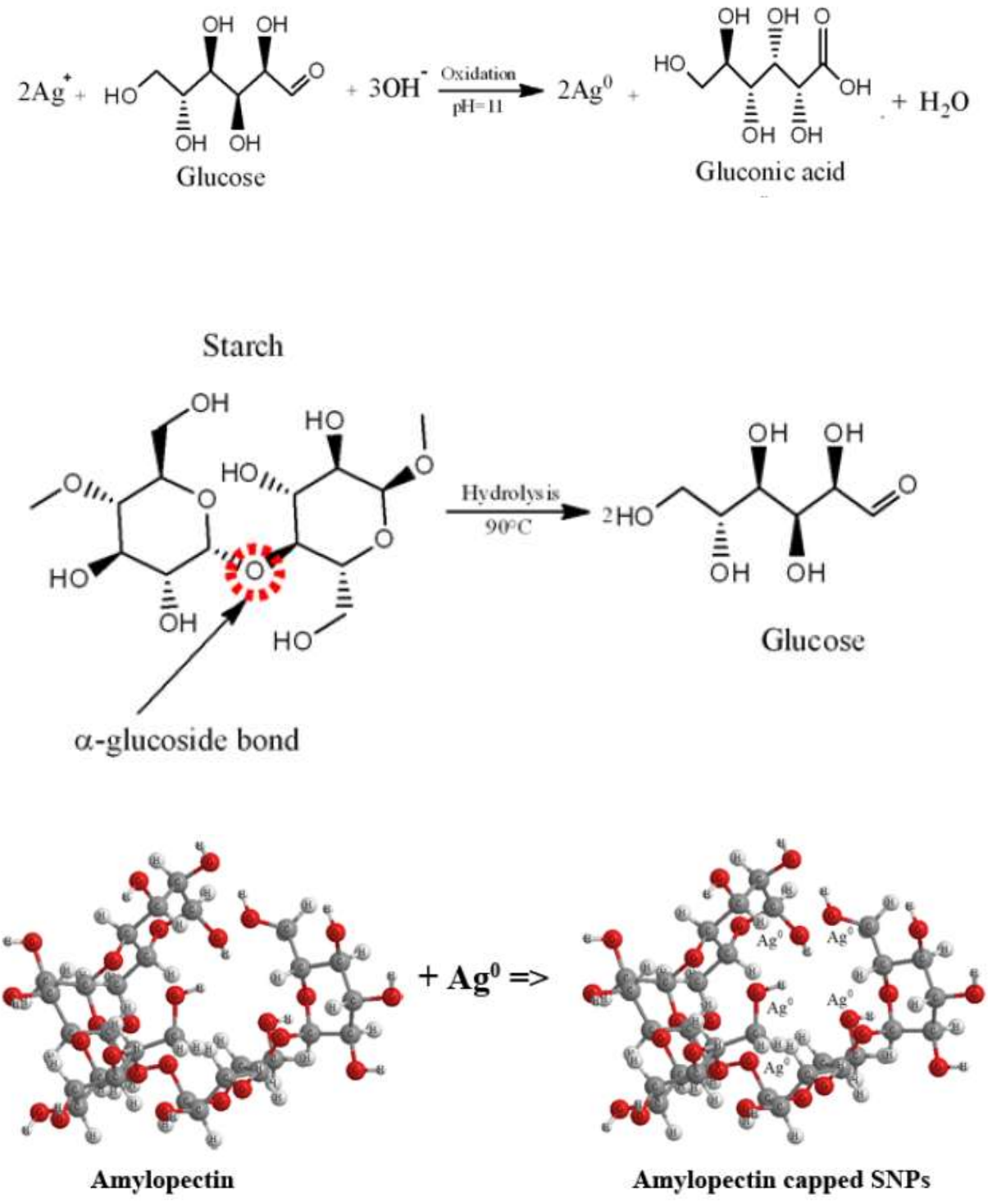

Figure 4.4: Proposed Mechanism of Starch-Silver Nanoparticles

4.5 Inhibition Study

From the respective gravimetric data, the result of the inhibition study is represented with a plot (Figure 4.5, 4.6 and 4.7) showing the inhibitory properties of starch-silver nanoparticles, honey and starch-silver nanoparticles in combination with 5 cm^3 of honey.

4.6 Synergism Evaluation

The result from the synergism parameters (which is represented in figure 4.8) derived from the gravimetric data is used to observe the effect of honey, its interaction with starch-Silver nanoparticles and its synergistic and antagonistic behavior.

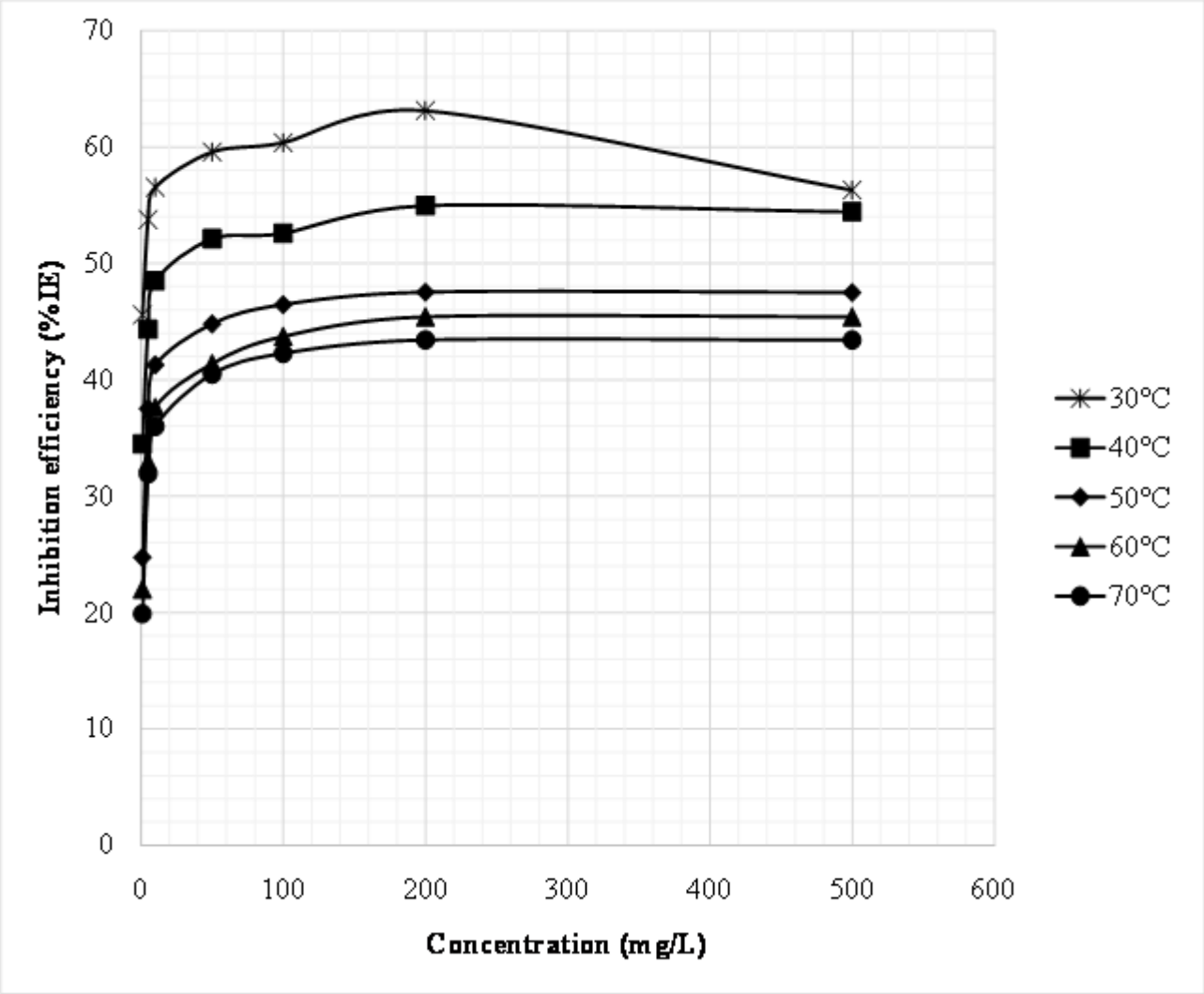

Figure 4.5: Plot of Inhibition Efficiency (%IE) for Mild Steel in 0.5 M HCl in the Presence of Varying Concentration of starch-AgNPs at (30^{o}C, 40^{o}C, 50^{o}C, 60^{o}C and 70^{o}C) from Weight Loss Measurement

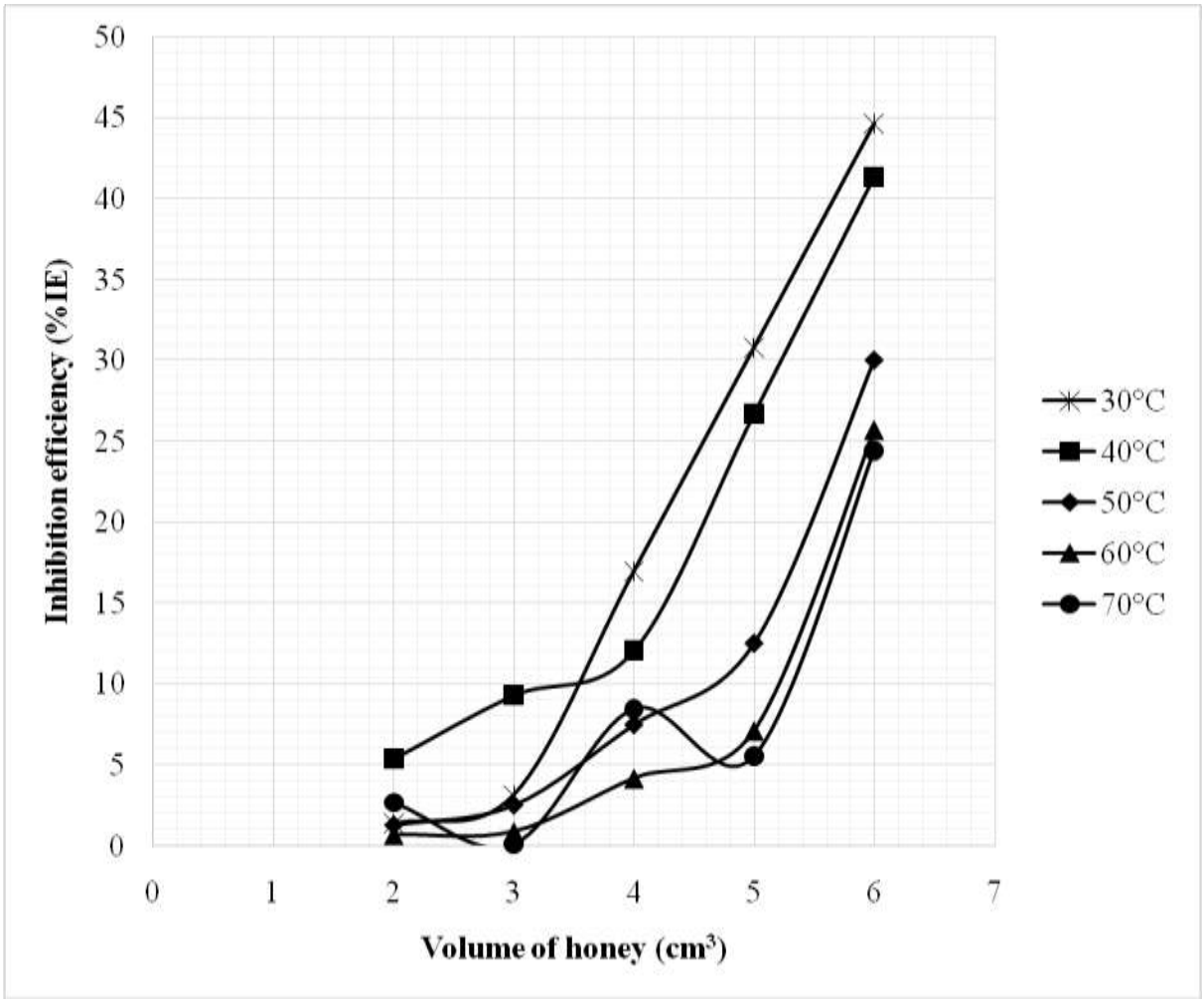

Figure 4.6: Inhibition Efficiency (%IE) for Mild Steel in 0.5 M HCl in the Absence and the Presence of Varied Concentration of Honey at (30^{o}C, 40^{o}C, 50^{o}C, 60^{o}C and 70^{o}C) from Weight Loss Measurement

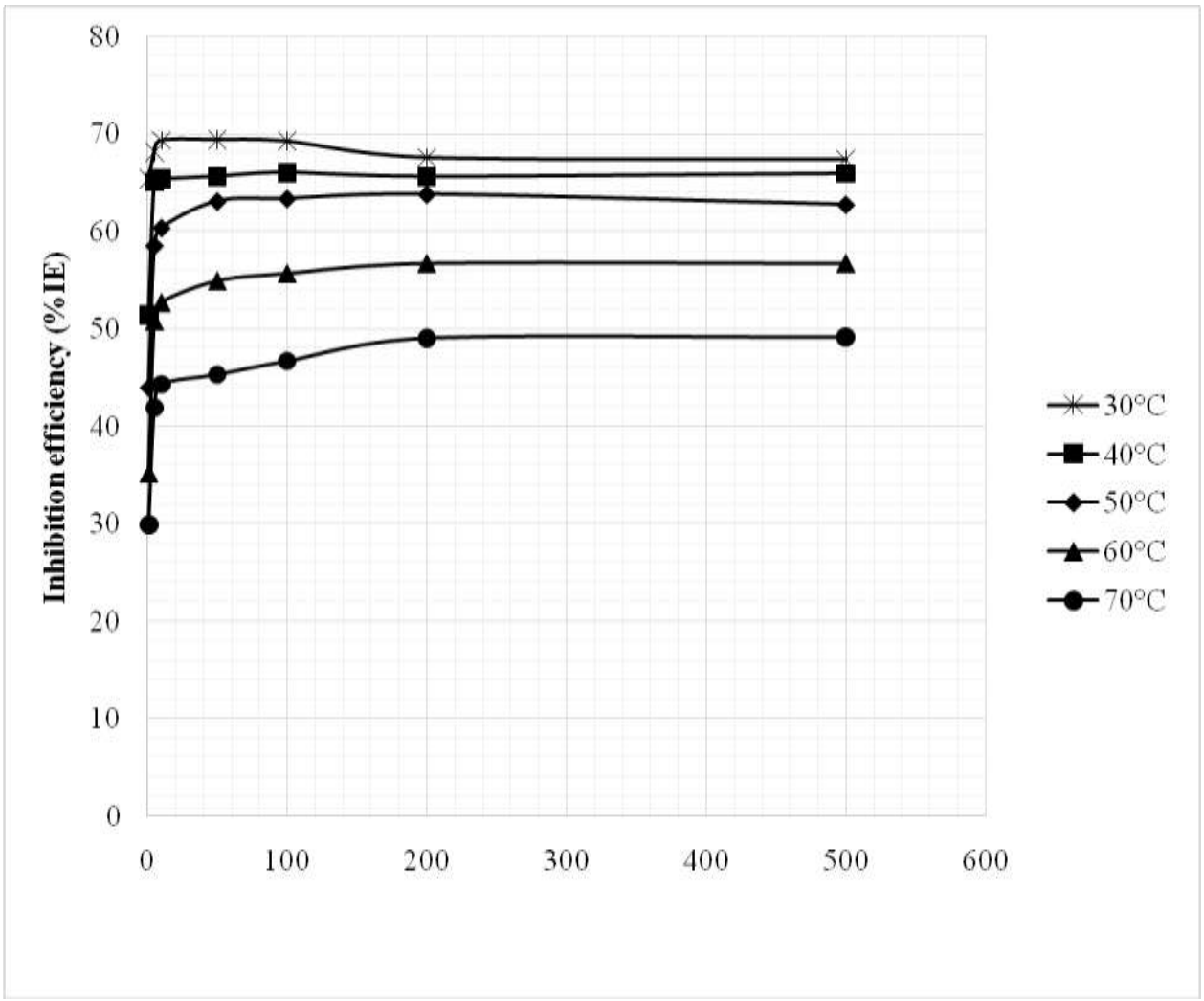

Figure 4.7: Plot of Inhibition Efficiency (%IE) for Mild Steel in 0.5 M HCl in the Presence of Varying Concentration of starch-AgNPs with 5 cm^3 honey at (30^oC, 40^oC, 50^oC, 60^oC and 70^oC) from Weight Loss Measurement

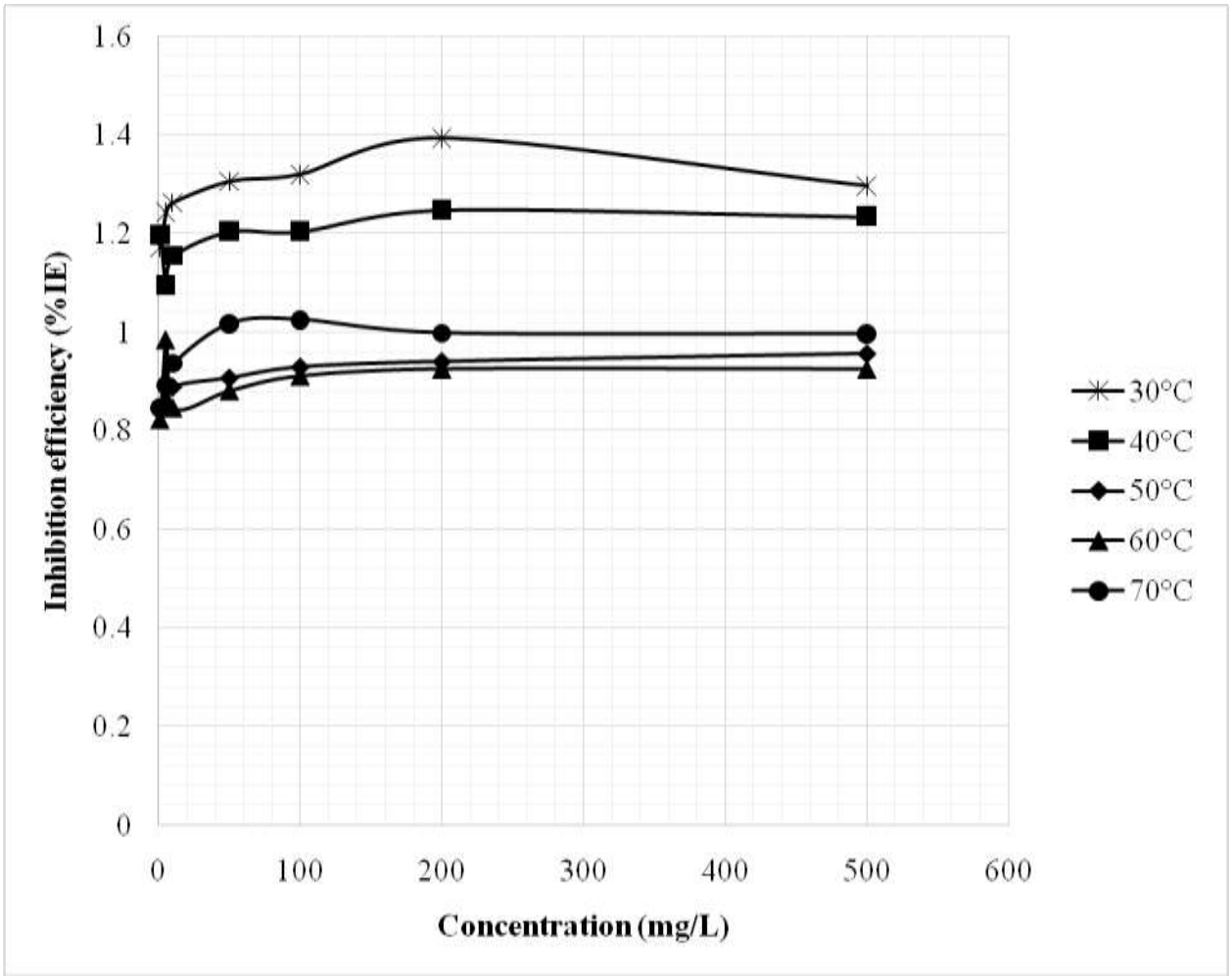

Figure 4.8: Plot of Synergism Parameter (S_1), for Mild Steel in 0.5 M HCl in the Absence and Presence of Varying Concentration of Starch-AgNPs with 5 cm^3 Honey at (30^oC, 40^oC, 50^oC, 60^oC and 70^oC) from Weight Loss Measurement

4.7 Adsorption Evaluation

The character of adsorption of starch-AgNPs alone and starch-AgNPs in combination with honey was elucidated from the values of degree of surface coverage (θ); $\theta = \frac{CRo - CRi}{CRo}$ calculated from the weight loss data. The plot of C/θ against C for starch-silver nanoparticles and starch-silver nanoparticles in combination with honey is shown in figure 4.9 and 4.1.0 respectively which is characteristics of Langmuir adsorption isotherm given by equation:

$$\frac{C}{\theta} = \frac{1}{k} + C$$

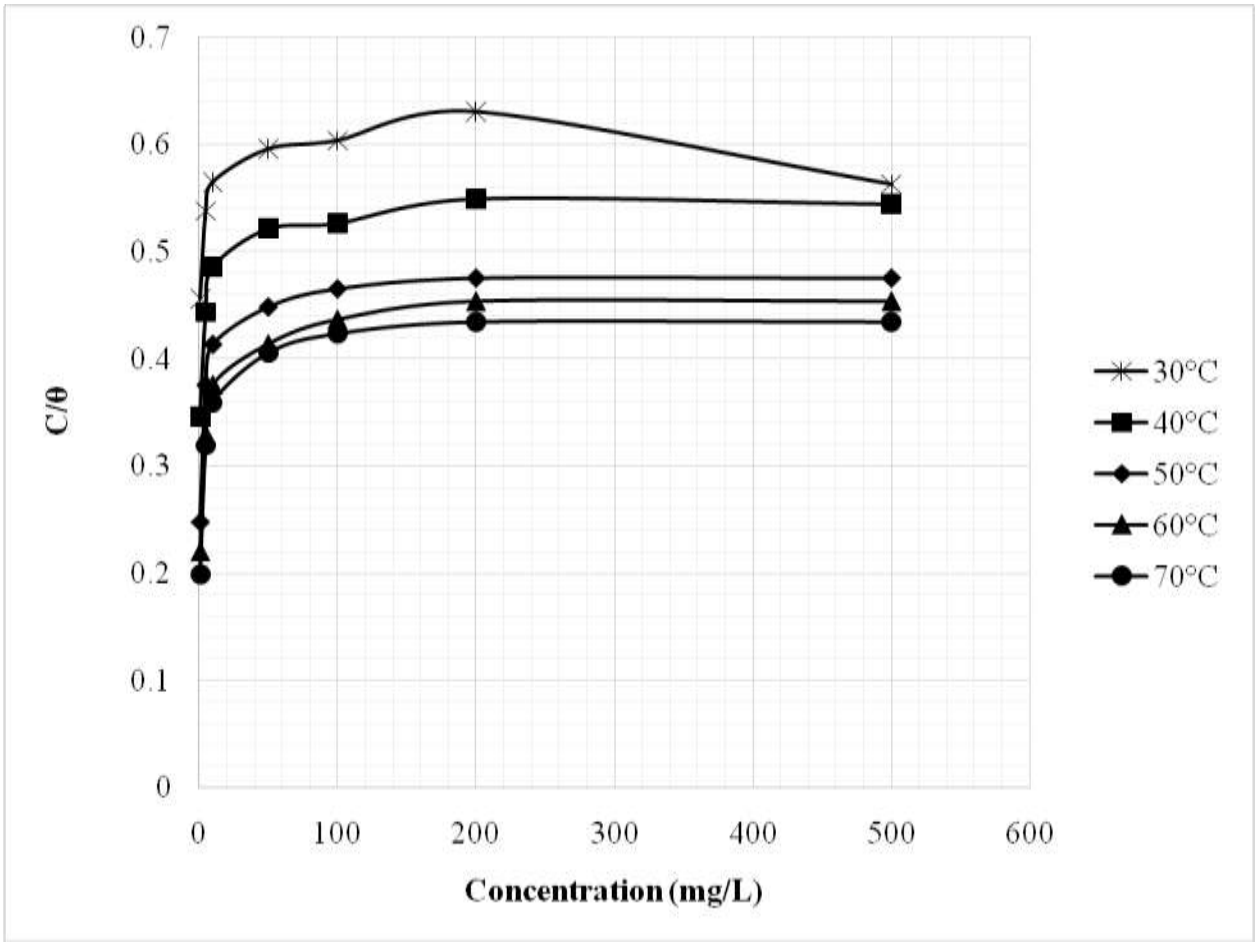

Figure 4.9: Adsorption Evaluation for Mild Steel in 0.5 M HCl in the Presence of Varying Concentration of Starch-AgNPs at (30^{o}C, 40^{o}C, 50^{o}C, 60^{o}C and 70^{o}C) from Weight Loss Measurement

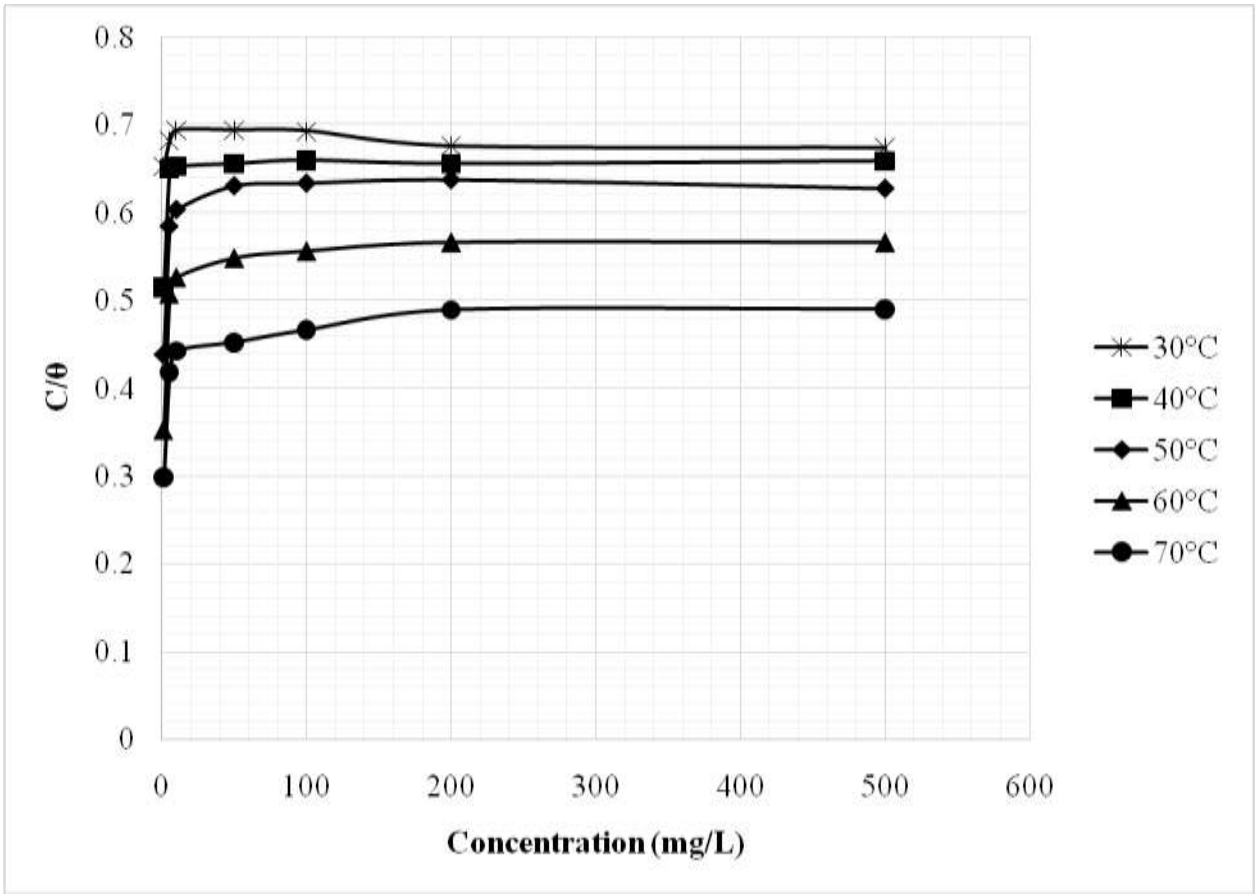

Figure 4.1.0: Adsorption Evaluation, for Mild Steel in 0.5 M HCl in the Presence of Varying Concentration of Starch-AgNPs with 5 cm^3 Honey at (30°C, 40°C, 50°C, 60°C and 70°C) from Weight Loss Measurement

CHAPTER FIVE

5.0 DISCUSSION

5.1 Analysis of Silver Nanoparticles Preparation

It is well known that silver nanoparticles exhibits yellowish-brown colour in aqueous state thus, the brown colouration observed from the synthesized composites can be attributed to the excitation of surface plasmon vibrations in the metal nanoparticles (Shankar *et al.*, 2004). The reduction of the metal ion can be easily observed by the colour change of the mixture which is turned from colourless to dark brown, suggesting complete reduction of the nanoparticles (Yakout, 2015). This also, corresponds to reports from previous literatures (Mulvaney, 1996). The composite is made visible in plate I and II.

5.2 Corrosion Analysis

Corrosion inhibition of mild steel using starch-silver nanoparticles and honey in 0.5 M HCl was investigated in this study using weight loss technique. From the data, it can be seen that the corrosion rate decreased in the presence of inhibitor (AgNPs) in contrast to that of the blank solution (acid), at each of the temperature level. Also the corrosion rate increased with increase in temperature at all concentrations. This corresponds to reports in previous literatures. (Mobin, 2011). The result from the gravimetric data reveals that the steel was more corroded, as the surface was more rough in the blank medium. The results further suggest that the presence of inhibitor reduced the extent of corrosion, the surface became smoother compared to the sample in the uninhibited solution. This reveals the performance of inhibitor by protective layer formation; which separates the interaction between the metal and corrosive medium. Similar behavior was observed by Kadhum *et al.*, 2014.

5.3.0 Characterization

5.3.1 UV-Visible Analysis

The bio-reduced sample was confirmed using UV-Visible spectrophotometer. The obtained AgNPs was purified through repeated centrifugation for 20 minutes and washed with distilled water (Yakout and Mostafa, 2015). The sample was analyzed by preparing dilute solution made in deionized water. The reduction of silver ions was monitored from 300 – 800 nm with deionized water serving as blank. Metallic nanoparticles display characteristic optical absorption spectra in the UV– visible region called Surface Plasmon Resonance (SPR). The physical origin of light absorption of metallic nanoparticle is the coherent oscillation of conduction electron induced by the interacting electromagnetic field (Kreibig and Vollmer, 1995). When a small spherical metallic nanoparticle is irradiated by light, the oscillating electric field causes the oscillation of conduction electron to oscillate coherently. When electron cloud is displaced relative to the nuclei a restoring force initiates a coulomb attraction between electrons and nuclei that results in oscillation of electron cloud relative to the nuclear framework. These resonance is known as SPR and are actually small particle effect since they are absent in their individual atom, as well as in their bulk. The broadening of the peak at that wavelength is attributed to the formation of polydispersed silver nanoparticles (Obot *et al*., 2013). Figure 4.1 shows UV-Vis spectrum recorded from the composite AgNPs. Corresponding with what was recorded in previous literature. All the solutions exhibited characteristic silver surface plasmon resonance (SPR) typically located in between 410-425 nm. The absorbance peak was recorded at 415 nm which corresponds to that of AgNPs; 410 – 430 nm (Yakout and Mostafa, 2015).

5.3.2 Fourier Transform Infrared Spectroscopy (FTIR) Spectra Analysis

Fourier Transform Infrared Spectroscopy (FTIR) measures the molecular vibration, determines the functional group present and the molecular structure of the compound (He *et al*., 2007; Mallakpour and Dinari, 2011). The FTIR Spectra of the composite was carried out to identify the possible functional groups responsible for the reduction of the silver ions and capping of the bioreduced silver nanoparticles synthesized by starch and also to monitor the functional groups' interaction of starch with silver nanoparticles. The FTIR spectra of starch and starch-AgNPs are shown in figure 4.2 and 4.3 respectively. From the spectra, the successful oxidation of aldehyde in figure 4.2 to carboxylic in figure 4.3 is conspicuously visible. From figure 4.2, C-H stretching of aldehyde was observed at wave number 2926.0 cm^{-1} while, the peak observed at 1636.3 cm^{-1} is indicative of C=O stretching of aldehyde and the peak noted at 1338.1 cm^{-1} suggests the C-H bending of aldehyde. On the other hand, the functional group observed from the spectrum in figure 4.3 explicates the successful redox reaction. The sharp peak observed at 1304.6 cm^{-1} is indicative of –C–O Carboxylic stretching. Also, at 1725.3 cm^{-1}, –C=O carboxylic stretch can be observed. Finally, the broad stretch observed at 3306.1 cm^{-1} is a characteristic feature of carboxylic –OH. This further justifies the oxidation of aldehyde in starch to carboxylic acid which corresponds to what was reported in previous literature (Manno *et al*., 2008). It is believed that extensive number of hydroxyl groups present in soluble starch facilitates the complexation of silver ions to the molecular matrix while the aldehyde terminals helped in reduction of the same (Vigneshwaran *et al*., 2006). As the reaction mixtures consist stoichiometrically equal number of silver ions; therefore, with an increase in starch concentration, the quantitatively increase in number of hydroxyl groups occurs. This facilitates

the reduction of silver ions by electrostatic binding in the helical structure of the starch, and thereby promotes the formation of AgNPs (Gao *et al*., 2011). The obtained FTIR spectra are consistent with previously reported literature.

5.3.3 SEM Analysis for Starch-Silver nanoparticles

Plate III, IV, V and VI are visible observation of the SEM morphology of silver nanoparticles after reaction with starch. The black spots represent pinholes in their surfaces, where no starch had been deposited through replacement reaction (Xia and Sun, 2009). It is believed that the existence of such pinholes allows for the in and out transportation of chemical species. The location of these black spots implied that the replacement reaction occurred on the surface which corresponds to that of previously reported literature (Xia and Sun, 2009).

5.3.4 Mechanism of Starch-Silver Nanoparticles Analysis

The gelatinization process of Starch using boiling water enhanced and improved the hydrolysis of Starch amylose content. This will be followed by the dissociation of oxidized Starch molecules into glucose units (Uthumporn *et al*., 2012). The reduction of Ag^{+} ions was done by the glucose units which contain a carbonyl group named aldehyde, that is responsible for the reduction of Ag^{+} ions to Silver nanoparticles (Ag^{o}) (Kumar *et al*., 2014). This is consistent with the mechanism proposed by Shervani and Yamamto (2011), where Ag_2O molecules dissociate into silver ions (Ag^{+}), which subsequently get reduced to Silver nanoparticles (Ag^{o}) in the presences of the electron pairs produced from Starch fragment oxidation. In addition, the synthesized nanoparticles could be stabilized by the helical amylopectin residue of Starch molecules as shown in the proposed reaction mechanism shown in figure 4.4 forming starch-Ag nanocomposite. Hence, the Starch acts not only as a reducing agent in an alkaline medium, but also as a capping (stabilising) agent (Salaheldin, 2018).

The reduction of silver ions is coupled to the oxidation of sugar molecules by the reaction of a terminal aldehyde to a carboxylic acid (Bel *et al.*, 2015). The possible equation of the reaction is shown below:

$R\text{-}CH{=}O + 2[Ag{+}OH^{-}] \rightarrow R\text{-}C(OH){=}O + 2Ag + H_2O$

5.4 Inhibition Analysis

The plot of inhibiton efficiency for starch-AgNPs, honey and starch-AgNPs in combination with honey (Figure 4.5, 4.6 and 4.7 respectively) as a function of concentration at varied temperature also reveals that inhibiton efficiency increases with increase in concentration of the test sample showing a maximum efficiency of 63.136% at 30^{o}C temperature in presence of starh-AgNPs concentration of 200 mg/l; it was observed that, further addition of starch does not significantly influence the inhibition efficiency. However, a maximum efficiency of 44.656 % at 30 ^{o}C (6 cm^{3}) was observed in the solution containing honey alone. It was further observed that, the combination of starch-AgNPs with honey further improved the inhibition efficiency as a maximum efficiency of 69.444 % at 30 ^{o}C (50 mg/l) was recorded. A decrease in inhibition efficiency with increasing temperature suggests possible desorption of some of the adsorbed molecules from the metal surface at higher temperatures. This behavior suggests physical adsorption on the metal surface (Oguzie, 2004). As the temperature increases, the quantity of equilibrium of adsorption decreases and as a result, the plot of higher temperatures is below the lower ones. The data derived from the weight loss measurement suggests that it is an adsorption inhibitor and the adsorption inhibition process occurs physically on the metal surface since the inhibition efficiency of starch-AgNPs for mild steel corrosion decreases with increase in temperature. Figure 4.5, 4.6 and 4.7 shows that starch and honey were physically adsorbed on the steel surface since the plots of higher temperatures are under that of lower ones (Mobin *et al.*,

2011). The inhibition of mild steel corrosion in the presence of starch-AgNPs could be attributed to the adsorption of the compound on to mild steel surface, which blocks the metal and thus, do not permit the corrosion process to take place (Mobin *et al.*, 2011).

The decrease in inhibition efficiency with increasing temperature may be due to the fact that most of the effects at elevated temperatures are adverse to corrosion inhibition by increasing the corrosion rate and decreasing the tendency of the starch to be adsorbed on the steel surface (Mobin *et al.*, 2011). The increased inhibition efficiency with increasing starch concentration indicates that more inhibitor molecules are adsorbed on the steel surface leading to the formation of a protective film (Rao and Singhal, 2009). In addition, the binding interactions between starch and silver nanoparticle are weak and can be reversible at higher temperatures, allowing separation of the synthesized particles (Yakout and Mostafa, 2015).

5.5 Synergism Analysis

To observe the effect of honey on the corrosion inhibition behavior of starch-AgNPs, the corrosion of mild steel in 0.5 M HCl in absence and presence of varying concentration of the starch-AgNPs in combination with honey (5 cm^3) was separately studied in the temperature range of 30^oC, 40^oC, 50^oC, 60^oC and 70^oC by weight loss technique. The results from the gravimetric data were recorded. It was observed that the corrosion rates of mild steel in 0.5 M HCl in presence of starch-AgNPs in combination with honey are further reduced in comparison to that of starch-AgNPs or honey alone. Figure 4.8 reveals the plot of synergism parameter (S_1), for mild steel in 0.5 M HCl in the absence and presence of varying concentration of starch-AgNPs with 5 cm^3 honey at (30^{o}c, 40^{o}c, 50^{o}c, 60^{o}c and 70^{o}c) from weight loss measurement.

S_1 Approaches 1 when no interaction between inhibitor (starch-AgNPs) and the honey exist, whereas $S_1>1$ indicate a synergistic effect. In the case of $S_1<1$, antagonistic behavior prevails

which may be attributed to competitive adsorption (Mobin *et al.*, 2011). The values of the synergism parameter for the various concentrations of starch studied were calculated from the gravimetric data at 30°C, 40°C, 50°C, 60°C and 70°C and the results were presented. The synergism parameter S_1 is found to be greater than unity at lower temperature and higher concentration indicating that the enhanced inhibition efficiency caused by the addition of honey is only due to synergism (Mobin *et al.*, 2011).

5.6 Adsorption Analysis

The adsorption of organic compounds on metal surfaces can be described by two main types of interactions namely, physical adsorption and chemical adsorption. These adsorptions are dependent on the electronic structure of the metal, the nature of the electrolyte and the chemical structure of the organic compound (Mobin *et al.*, 2011). The character of adsorption of starch alone and starch in combination with honey was elucidated from the values of degree of surface coverage (θ) calculated from the weight loss data. The results recorded from the adsorption study are representative of the adsorption effect in the presence of starch-AgNPs alone and the synergism of starch-AgNPs with honey respectively. The plot of C/θ against C for starch-silver nanoparticles and starch-silver nanoparticles in combination with honey is shown in figure 4.9 and 4.1.0 respectively which is characteristics of Langmuir adsorption isotherm given by equation:

$$\frac{C}{\theta} = \frac{1}{k} + C$$

Where, θ is the degree of surface coverage, K is the equilibrium constant of the adsorption process and C is the starch concentration. From the plots in figure 4.4 and 4.5, it can be observed that at higher concentration of inhibitor, the adsorption is improved. Also, the addition of 5 cm^3 of honey further improves the adsorption of the nanoparticles on the mild steel (Mobin

et al., 2011). Furthermore, as the temperature increases, the quantity of equilibrium of adsorption decreases which corresponds to studies reported in previous literatures (Ebenso *et al.*, 1999).

CHAPTER SIX

6.0 Conclusion and Recommendation

6.1 Conclusion

This study showed that starch-AgNPs acts as a good capping agent and inhibitor of mild steel corrosion in acidic medium. The colour change of the composite mixture from colourless to reddish brown corresponding to what was reported in previous studies on nanoparticles, is indicative of the complete reduction of the starch-AgNPs. From the FTIR spectra, it was observed that the monomers of starch are excellent reducing agent. The data derived from the weight loss measurement suggests that it is an adsorption inhibitor and the adsorption inhibition process occurs physically on the metal surface since the inhibition efficiency of starch-AgNPs for mild steel corrosion decreases with increase in temperature. It was also seen that the binding interactions between starch and AgNPs are weak and as such dissociates at higher temperature, allowing the separation of the synthesized particles. The characterization with UV-Visible confirms the adsorption peak (λ_{max}) of AgNPs at 415 nm which correlates with reports from previous studies. The results do support the claim; Starch-AgNPs is a good inhibitor for the corrosion of mild steel and the addition of honey further improved the inhibition efficiency of the inhibitor.

6.2 Recommendation

It is recommended that:

- Chemometrics prediction, classification and cross validation of data in nanoparticles synthesis should be encouraged to save cost of analysis and for alternative data interpretation.
- More green inhibitors and alternative technigues should be researched upon as viable raw materials and methods in inhibition of corrosion of mild steel.
- More synergistic studies on green renewable inhibitors are recommended for alternative and improved corrosion inhibition of mild steel.

REFERENCES

Abdallah, M. (2004). Antibacterial drugs as corrosion inhibitors for corrosion of aluminium in hydrochloric solution. *Corrosion Science*, *46*(8), 1981-1996.

Adams, F. C., and Barbante, C. (2013). Nanoscience, nanotechnology and spectrometry. *Spectrochimica Acta Part B: Atomic Spectroscopy*, *86*, 3-13.

Acharya, S., and Upadhyay, S. N. (2004). The inhibition of corrosion of mild steel by some fluoroquinolones in sodium chloride solution. *TRANSACTIONS-INDIAN INSTITUTE OF METALS*, *57*(3), 297-306.

Ahmad, Z. (2006). *Principles of corrosion engineering and corrosion control*. Elsevier.

Ali, S. A., Saeed, M. T., and Rahman, S. U. (2003). The isoxazolidines: a new class of corrosion inhibitors of mild steel in acidic medium. *Corrosion Science*, *45*(2), 253-266.

Alvarez, M. G., and Galvele, J. R. (1976). Pitting of high purity zinc and pitting potential significance. *Corrosion*, *32*(7), 285-294.

ASTM Committee G-1 on Corrosion of Metals. (1999). *Standard practice for preparing, cleaning, and evaluating corrosion test specimens*. *Journal of Applied Polymer Science*, **121**:16-18.

Bajwa, R. S., Yaldram, K., and Rafique, S. (2013). A scientometric assessment of research output in nanoscience and nanotechnology: Pakistan perspective. *Scientometrics*, *94*(1), 333-342.

Ball, D. W. (2007). The chemical composition of honey. *Journal of chemical education*, *84*(10), 1643.

Balasubramaniam, R. (2009). *Callister's Materials Science and Engineering: Indian Adaptation (W/Cd)*. John Wiley and Sons.

Barber, D. J., and Freestone, I. C. (1990). An investigation of the origin of the colour of the Lycurgus Cup by analytical transmission electron microscopy. *Archaeometry*, *32*(1), 33-s45.

Baker, R., Hu, X., Neville, A., and Cushnaghan, S. (2011). Flow-induced corrosion and erosion-corrosion assessment of carbon steel pipework in oil and gas production. *CORROSION 2011*.

Bautista, A. (1996). Filiform corrosion in polymer-coated metals. *Progress in Organic Coatings*, *28*(1), 49-58.

Bell, N. S., Dunphy, D. R., Lambert, T. N., Lu, P., and Boyle, T. J. (2015). In situ characterization of silver nanoparticle synthesis in maltodextrinsupramolecular structures. *Colloids and Surfaces B: Biointerfaces*, *134*, 98-104.

Bogdanov, S. (2012). Honey as nutrient and functional food. *Proteins*, *1100*, 1400-2700.

Bou-Saleh, Z., Shahryari, A., and Omanovic, S. (2007). Enhancement of corrosion resistance of a grade 316LVM stainless steel by potentiodynamic cyclic polarization. *Thin Solid Films*, *515*(11), 4727-4737.

Bradlee E., 2003. *Corrosion and protection-Engineering materials and processes*, chapter 7.6, Springer- Verlag, London

Buzea, C., Pacheco, L.,and Robbie, K. (2007). Nanomaterials and Nanoparticles: Sources and Toxicity. *Journal of Applied Polymer Science*, 121: 1458–1465.

Castle, J. E., and Asami, K. (2004). A more general method for ranking the enrichment of alloying elements in passivation films. *Surface and Interface Analysis: An International Journal devoted to the development and application of techniques for the analysis of surfaces, interfaces and thin films*, *36*(3), 220-224.

Castle, J. E., and Qiu, J. H. (1990). The Application of ICP-MS and XPS to Studies of Ion Selectivity during Passivation of Stainless Steels. *Journal of The Electrochemical Society*, *137*(7), 2031-2038.

Chelikowsky, J. R., and Ratner, M. A. (2001). Guest Editors' Introduction: Nanoscience, Nanotechnology, and Modeling. *Computing in Science and Engineering*, *3*(4), 40-41.

Cheng, W., and Compton, R. G. (2014). Electrochemical detection of nanoparticles by 'nano-impact'methods. *TrAC Trends in Analytical Chemistry*, *58*, 79-89.

Chimentao, R. J., Kirm, I., Medina, F., Rodriguez, X., Cesteros, Y., Salagre, P., and Sueiras, J. E. (2004). Different morphologies of silver nanoparticles as catalysts for the selective oxidation of styrene in the gas phase. *Chemical Communications*, (7), 846-847.

Cobb, H. M. (2010). *The history of stainless steel*. ASM International.

Colvin, V. L. (2003). The potential environmental impact of engineered nanomaterials. *Nature biotechnology*, *21*(10), 1166.

Dreher, K. L. (2004). Health and environmental impact of nanotechnology: toxicological assessment of manufactured nanoparticles. *Toxicological Sciences*, *77*(1), 3-5.

Drexler, K. E. (1986). Engines of Creation: The Coming Era of Nanotechnology and Nanosystems: Molecular Machinery, Manufacturing, and Computation.

Ebenso, E. E., Ekpe, U. J., Ita, B. I., Offiong, O. E., and Ibok, U. J. (1999). Effect of molecular structure on the efficiency of amides and thiosemicarbazones used for corrosion inhibition of mild steel in hydrochloric acid. *Materials chemistry and physics*, *60*(1), 79-90.

El Badawy, A. M., Silva, R. G., Morris, B., Scheckel, K. G., Suidan, M. T., and Tolaymat, T. M. (2010). Surface charge-dependent toxicity of silver nanoparticles. *Environmental science and technology*, *45*(1), 283-287.

El-Nour, K. M. A., Eftaiha, A. A., Al-Warthan, A., and Ammar, R. A. (2010). Synthesis and applications of silver nanoparticles. *Arabian journal of chemistry*, *3*(3), 135-140.

Ernst, P., and Newman, R. C. (2002). Pit growth studies in stainless steel foils. I. Introduction and pit growth kinetics. *Corrosion Science*, *44*(5), 927-941.

Evanoff Jr, D. D., and Chumanov, G. (2005). Synthesis and optical properties of silver nanoparticles and arrays. *ChemPhysChem*, *6*(7), 1221-1231.

Evans, U. R. (1960). The Corrosion and. *Passivity, and Protection of Metals [in Russian], Metallur*.

Evans, U. R., and Taylor, C. A. J. (1972). Mechanism of atmospheric rusting. *Corrosion Science*, *12*(3), 227-246.

Fanta, G. F., Felker, F. C., & Shogren, R. L. (2002). Formation of crystalline aggregates in slowly-cooled starch solutions prepared by steam jet cooking. *Carbohydrate Polymers*, *48*(2), 161-170.

Ferrari, M. (2005). Cancer nanotechnology: opportunities and challenges. *Nature reviews cancer*, *5*(3), 161.

Fisher, K., Wallén, E., Laenen, P. P., and Collins, M. (2006). Battery waste management life cycle assessment. *Environmental Resources Management ERM, Ltd*.

Fontana, M. G., Greene, N. D., and Mcdonald, D. D. (1979). Corrosion engineering. *Journal of The Electrochemical Society*, *126*(6), 232C-232C.

Frankel, G. S. (1998). Pitting corrosion of metals a review of the critical factors. *Journal of the Electrochemical Society*, *145*(6), 2186-2198.

Frankel, G. S., Stockert, L., Hunkeler, F., and Boehni, H. (1987). Metastable pitting of stainless steel. *Corrosion*, *43*(7), 429-436.

Fuller, S. B., Wilhelm, E. J., and Jacobson, J. M. (2002). Ink-jet printed nanoparticle microelectromechanical systems. *Journal of Microelectromechanical systems*, *11*(1), 54-60.

Frattini, A., Pellegri, N., Nicastro, D., and De Sanctis, O. (2005). Effect of amine groups in the synthesis of Ag nanoparticles using aminosilanes. *Materials Chemistry and Physics*, *94*(1), 148-152.

Gao, X., Wei, L., Yan, H., and Xu, B. (2011). Green synthesis and characteristic of core-shell structure silver/starch nanoparticles. *Materials Letters*, *65*(19-20), 2963-2965.

Geethalakshmi, R., and Sarada, D. V. L. (2010). Synthesis of plant-mediated silver nanoparticles using Trianthema decandra extract and evaluation of their anti microbial activities. *International Journal of Engineering Science and Technology*, *2*(5), 970-975.

Grundmeier, G., Schmidt, W., and Stratmann, M. (2000). Corrosion protection by organic coatings: electrochemical mechanism and novel methods of investigation. *Electrochimica Acta*, *45*(15-16), 2515-2533.

Gurunathan, S., Kalishwaralal, K., Vaidyanathan, R., Venkataraman, D., Pandian, S. R. K., Muniyandi, J., and Eom, S. H. (2009). Biosynthesis, purification and characterization of silver nanoparticles using Escherichia coli. *Colloids and Surfaces B: Biointerfaces*, *74*(1), 328-335.

Haynes, C. L., and Van Duyne, R. P. (2001). Nanosphere lithography: a versatile nanofabrication tool for studies of size-dependent nanoparticle optics.

He, Y., Du, Z., Lv, H., Jia, Q., Tang, Z., Zheng, X., and Zhao, F. (2013). Green synthesis of silver nanoparticles by Chrysanthemum morifolium Ramat. extract and their application in clinical ultrasound gel. *International journal of nanomedicine*, *8*, 1809.

He, B., Tan, J. J., Liew, K. Y., and Liu, H. (2004). Synthesis of size controlled Ag nanoparticles. *Journal of Molecular Catalysis A: Chemical*, *221*(1-2), 121-126.

Herting, G. (2008). *Bioaccessibility of Stainless Steels: Importance of Bulk and Surface Features* (Doctoral dissertation, KTH).

Hong, T., Ogushi, T., and Nagumo, M. (1996). The effect of chromium enrichment in the film formed by surface treatments on the corrosion resistance of type 430 stainless steel. *Corrosion science*, *38*(6), 881-888.

Hughes, M. P. (2000). AC Electrokinetics: application for nanotechnology. Nanotechnology, 11(2), 124.

James, A.O., Oforka, N.C., Abiola, O.K., and Ita, B.I. (2007). A Study

On Inhibition of Mild Steel Corrosion in Hydrochloric Acid by PyrydoxolHydrochloride. *Scielo Analytics*,**32**(3): 1678-4618.

Jang, E. J., Kim, S. S., Cho, K. A., and Kim, H. S. (2006). *U.S. Patent No. 7,042,003*. Washington, DC: U.S. Patent and Trademark Office.

Jeng, H. A., and Swanson, J. (2006). Toxicity of metal oxide nanoparticles in mammalian cells. *Journal of Environmental Science and Health Part A*, *41*(12), 2699-2711.

Jiang, L., Zhao, Y., and Zhai, J. (2004). A lotus-leaf-like superhydrophobic surface: a porous microsphere/nanofiber composite film prepared by electrohydrodynamics. *Angewandte Chemie*, *116*(33), 4438-4441.

Jones, D. A. (1996). Principles and Prevention of Corrosion, 2nd. *Ed. Upper Saddle River, NY: Prentice Hall*, 168-198.

Kadhum, A. A. H., Mohamad, A. B., Hammed, L. A., Al-Amiery, A. A., San, N. H., and Musa, A. Y. (2014). Inhibition of mild steel corrosion in hydrochloric acid solution by new coumarin. *Materials*, *7*(6), 4335-4348.

Kalra, Y. P. (1995). Determination of pH of soils by different methods: collaborative study. *Journal of AOAC International*, *78*(2), 310-324.

Khomutov, G. B., and Gubin, S. P. (2002). Interfacial synthesis of noble metal nanoparticles. *Materials Science and Engineering: C*, *22*(2), 141-146.

Kolawole, S. K., Kolawole, F. O., Enegela, O. P., Adewoye, O. O., Soboyejo, A. B. O., and Soboyejo, W. O. (2016). Pitting Corrosion of a Low Carbon Steel in Corrosive Environments: Experiments and Models. In *Advanced Materials Research* (Vol. 1132, pp. 349-365). Trans Tech Publications.

Kolotyrkin, J. M. (1963). Pitting corrosion of metals. *Corrosion*, *19*(8), 261t-268t.

Kolpak, A. M., Grinberg, I., and Rappe, A. M. (2007). Polarization effects on the surface chemistry of PbTiO 3-supported Pt films. *Physical review letters*, *98*(16), 166101.

Koseoglu-Imer, D. Y., Kose, B., Altinbas, M., and Koyuncu, I. (2013). The production of polysulfone (PS) membrane with silver nanoparticles (AgNP): physical properties, filtration performances, and biofouling resistances of membranes. *Journal of membrane science*, *428*, 620-628.

Kossmann, J., and Lloyd, J. (2000). Understanding and influencing starch biochemistry. *Critical Reviews in Plant Sciences*, *19*(3), 171-226.

Kreibig, U., and Vollmer, M. (1995). Theoretical considerations. In *Optical properties of metal clusters* (pp. 13-201). Springer, Berlin, Heidelberg.

Kruger, J. (1976). Passivity and its breakdown on iron and iron base alloys. In *USA-Japan Seminar, NACE, Houston TX* (Vol. 91).

Kumar, B., Smita, K., Cumbal, L., Debut, A., and Pathak, R. N. (2014). Sonochemical synthesis of silver nanoparticles using starch: a comparison. *Bioinorganic chemistry and applications*, *2014*.

Kumar, S., Baruah, A., Tonda, S., Kumar, B., Shankar, V., and Sreedhar, B. (2014). Cost-effective and eco-friendly synthesis of novel and stable N-doped ZnO/gC 3 N 4 core–shell nanoplates with excellent visible-light responsive photocatalysis. *Nanoscale*, *6*(9), 4830-4842.

Kumari, M., Mukherjee, A., and Chandrasekaran, N. (2009). Genotoxicity of silver nanoparticles in Allium cepa. *Science of the Total Environment*, *407*(19), 5243-5246.

Lakshmanan, G., Sathiyaseelan, A., Kalaichelvan, P. T., and Murugesan, K. (2018). Plant-mediated synthesis of silver nanoparticles using fruit extract of Cleome viscosa L.: Assessment of their antibacterial and anticancer activity. *Karbala International Journal of Modern Science*, *4*(1), 61-68.

Landolt, D. (2007). *Corrosion and surface chemistry of metals*. EPFL press.

Levard, C., Hotze, E. M., Lowry, G. V., and Brown Jr, G. E. (2012). Environmental transformations of silver nanoparticles: impact on stability and toxicity. *Environmental science and technology*, *46*(13), 6900-6914.

Li, Y., Wu, Y., and Ong, B. S. (2005). Facile synthesis of silver nanoparticles useful for fabrication of high-conductivity elements for printed electronics. *Journal of the American Chemical Society*, *127*(10), 3266-3267.

Little, B. J., and Lee, J. S. (2007). *Microbiologically influenced corrosion* (Vol. 3). John Wiley and Sons.

Love, J. C., Estroff, L. A., Kriebel, J. K., Nuzzo, R. G., and Whitesides, G. M. (2005). Self-assembled monolayers of thiolates on metals as a form of nanotechnology. *Chemical reviews*, *105*(4), 1103-1170.

Luo, X., Morrin, A., Killard, A. J., and Smyth, M. R. (2006). Application of nanoparticles in electrochemical sensors and biosensors. *Electroanalysis*, *18*(4), 319-326.

Machnikova, E., Whitmire, K. H., and Hackerman, N. (2008). Corrosion inhibition of carbon steel in hydrochloric acid by furan derivatives. *Electrochimica Acta*, *53*(20), 6024-6032.

Madhankumar, A., Nagarajan, S., Rajendran, N., and Nishimura, T. (2012). EIS evaluation of protective performance and surface characterization of epoxy coating with aluminum nanoparticles after wet and dry corrosion test. *Journal of Solid State Electrochemistry*, *16*(6), 2085-2093.

Mahgoub, F. M., and Al-Rashdi, S. M. (2016). Investigate the corrosion inhibition of mild steel in sulfuric acid solution by thiosemicarbazide. *Open J Phys Chem*, *6*, 54-66.

Mahmoud, B. A. A. (2012). *Assessment of Quality of Honey Obtained from Different Sources* (Doctoral dissertation, University of Gezira).

Mallakpour, S. and Dinari, M. (2011). Preparation and characterization of new organoclays using natural amino acids and Cloisite Na+. Applied Clay Science, 51, 353-359

Mankowski, J., and Szklarska-Smialowska, Z. (1977). The effect of specimen position on the shape of corrosion pits in an austenitic stainless steel. *Corrosion Science*, *17*(9), 725-735.

Mankowski, J., and Szklarska-Smialowska, Z. (1975). Studies on accumulation of chloride ions in pits growing during anodic polarization. *Corrosion Science*, *15*(6-12), 493-501.

Manno, D., Filippo, E., Di Giulio, M., & Serra, A. (2008). Synthesis and characterization of starch-stabilized Ag nanostructures for sensors applications. *Journal of Non-Crystalline Solids*, *354*(52-54), 5515-5520.

Miura, H., Miyao, N., Ogawa, H., Oda, K., Katsumura, M., and Mizutani, M. (2010). *U.S. Patent No. 7,662,207*. Washington, DC: U.S. Patent and Trademark Office.

Mobin, M., Khan, M. A., and Parveen, M. (2011). Inhibition of mild steel corrosion in acidic medium using starch and surfactants additives. *Journal of Applied Polymer Science*, *121*(3), 1558-1565.

Mohan, Y. M., Lee, K., Premkumar, T., and Geckeler, K. E. (2007). Hydrogel networks as nanoreactors: A novel approach to silver nanoparticles for antibacterial applications. *Polymer*, *48*(1), 158-164.

Molan, P. C. (2001). Honey as a topical antibacterial agent for treatment of infected wounds. *World Wide Wounds*, *1*, 1-13.

Moore, M. N. (2006). Do nanoparticles present ecotoxicological risks for the health of the aquatic environment?. *Environment international*, *32*(8), 967-976.

Moorthy, S. N. (2002). Physicochemical and functional properties of tropical tuber starches: a review. *Starch-Stärke*, *54*(12), 559-592.

Mnyusiwalla, A., Daar, A. S., and Singer, P. A. (2003). 'Mind the gap': science and ethics in nanotechnology. *Nanotechnology*, *14*(3).

Mulvaney, P. (1996). Surface plasmon spectroscopy of nanosized metal particles. *Langmuir*, *12*(3), 788-800.

Naixin, X., Zhao, L. Ding, C., Zhang, C., Li, R. and Zhong, Q. (2002). Laboratory observation of dew formation at early stage of atmospheric corrosion of metals. China Corros. Sci., 44:163-170

Neff, D., Bellot-Gurlet, L., Dillmann, P., Reguer, S., and Legrand, L. (2006). Raman imaging of ancient rust scales on archaeological iron artefacts for long-term atmospheric corrosion mechanisms study. *Journal of Raman Spectroscopy: An International Journal for Original Work in all Aspects of Raman Spectroscopy, Including Higher Order Processes, and also Brillouin and Rayleigh Scattering*, *37*(10), 1228-1237.

Noh, J. S., Laycock, N. J., Gao, W., and Wells, D. B. (2000). Effects of nitric acid passivation on the pitting resistance of 316 stainless steel. *Corrosion science*, *42*(12), 2069-2084.

Norin, M. (1998). *Groundwater and soil properties in an urban environment and their effects on the corrosion of soil buried constructions of carbon steel and zinc*. Chalmers University of Technology.

Obot, I.B., Umoren, S.A., and Johnson, A.S.(2013). Sunlight-mediated synthesis of silver nanoparticles using honey and its promising anticorrosion potentials for mild steel in acidic environments. *Journal of Material Environmental Science*, **4**(6): 1014-1018.

Obot, I. B., and Obi-Egbedi, N. O. (2010). Adsorption properties and inhibition of mild steel corrosion in sulphuric acid solution by ketoconazole: experimental and theoretical investigation. *Corrosion Science*, *52*(1), 198-204.

Oguzie, E.E. (2004). Evaluation of the inhibitory effect of methylene blue dye on the corrosion of aluminium in hydrochloric acid. *Journal of Material Chemistry and Physics*, **87**: 212-216.

Oguzie, E. E., Onuoha, G. N., and Onuchukwu, A. I. (2005). Inhibitory mechanism of mild steel corrosion in 2 M sulphuric acid solution by methylene blue dye. *Materials Chemistry and Physics*, *89*(2-3), 305-311.

Okafor, P. C., Ekpe, U. J., Ebenso, E. E., Oguzie, E. E., Umo, N. S., and Etor, A. R. (2006). Extract of Allium cepa and Allium sativum as corrosion inhibitors of mild steel in HCl solution. *Transactions of the SAEST*, *41*(2), 82-87.

Okamoto, G. (1973). Passive film of 18-8 stainless steel structure and its function. *Corrosion Science*, *13*(6), 471-489.

Oldfield, J. W. (1988). Electrochemical theory of galvanic corrosion. In *Galvanic Corrosion*. ASTM International.

Patil, R. S., Kokate, M. R., and Kolekar, S. S. (2012). Bioinspired synthesis of highly stabilized silver nanoparticles using Ocimum tenuiflorum leaf extract and their antibacterial activity. *Spectrochimica Acta Part A: Molecular and Biomolecular Spectroscopy*, *91*, 234-238.

Paul, L., and Machunda, R. L. (2016). Investigation of Aloe lateritia Gel as Corrosion Inhibitor for Mild Steel in 2 M HNO3 and 1 M H2SO4 Media. *Journal of Minerals and Materials Characterization and Engineering*, *4*(01), 33.

Pérez, S., and Bertoft, E. (2010). The molecular structures of starch components and their contribution to the architecture of starch granules: A comprehensive review. *Starch-Stärke*, *62*(8), 389-420.

Pistorius, P. C., and Burstein, G. T. (1992). Metastable pitting corrosion of stainless steel and the transition to stability. *Phil. Trans. R. Soc. Lond. A*, *341*(1662), 531-559.

Popova, A., Sokolova, E., Raicheva, S., and Christov, M. (2003). AC and DC study of the temperature effect on mild steel corrosion in acid medpria in the presence of benzimidazole derivatives. *Corrosion science*, *45*(1), 33-58.aa

Prasad, K. S., Pathak, D., Patel, A., Dalwadi, P., Prasad, R., Patel, P., and Selvaraj, K. (2011). Biogenic synthesis of silver nanoparticles using Nicotiana tobaccum leaf extract and study of their antibacterial effect. *African Journal of Biotechnology*, *10*(41), 8122-8130.

Raghavendra, G. M., Jung, J., and Seo, J. (2016). Step-reduced synthesis of starch-silver nanoparticles. *International journal of biological macromolecules*, *86*, 126-128.

Ramya, S., Anita, T., Shaikh, H., and Dayal, R. K. (2010). Laser Raman microscopic studies of passive films formed on type 316LN stainless steels during pitting in chloride solution. *Corrosion Science*, *52*(6), 2114-2121.

Rao, V. S., and Singhal, L. K. (2009). Corrosion behavior and passive film chemistry of 216L stainless steel in sulphuric acid. *Journal of materials science*, *44*(9), 2327-2333.

Rathish, R. J., Dorothy, R., Joany, R. M., and Pandiarajan, M. (2013). Corrosion resistance of nanoparticle-incorporated nano coatings. *European Chemical Bulletin*, *2*(12), 965-970.

Reardon, E. J. (1995). Anaerobic corrosion of granular iron: Measurement and interpretation of hydrogen evolution rates. *Environmental Science and Technology*, *29*(12), 2936-2945.

Revie, R. W. (2008). Corrosion and corrosion control: an introduction to corrosion science and engineering. John Wiley and Sons.

Rim-Rukeh, A., and Awatefe, J. K. (2006). Investigation of soil corrosivity in the corrosion of low carbon steel pipe in soil environment. *Journal of Applied Sciences Research*, *2*(8), 466-469.

Ring, S. G., Gee, J. M., Whittam, M., Orford, P., and Johnson, I. T. (1988). Resistant starch: its chemical form in foodstuffs and effect on digestibility in vitro. *Food chemistry*, *28*(2), 97-109.

Roberge, P. R. (2008). *Corrosion engineering: principles and practice* (Vol. 2). New York: McGraw-Hill.

Roberts, M. B., Atkins, C., Hogg, V., and Middleton, C. (2000). A proposed empirical corrosion model for reinforced concrete. *Proceedings of the Institution of Civil Engineers-Structures and Buildings*, *140*(1), 1-11.

Sadeghi, B. A. B. A. K. (2014). Green synthesis of silver nanoparticles using seed aqueous extract of Olea europaea. *International Journal of Nano Dimension*, *5*, 575-581.

Safaepour, M., Shahverdi, A. R., Shahverdi, H. R., Khorramizadeh, M. R., and Gohari, A. R. (2009). Green synthesis of small silver nanoparticles using geraniol and its cytotoxicity against fibrosarcoma-wehi 164. *Avicenna journal of medical biotechnology*, *1*(2), 111.

Saji, V. S., and Thomas, J. (2007). Nanomaterials for corrosion control. *Current Science*, 51-55.

Salaheldin, H. I. (2018). Optimizing the synthesis conditions of silver nanoparticles using corn starch and their catalytic reduction of 4-nitrophenol. *Advances in Natural Sciences: Nanoscience and Nanotechnology*, *9*(2), 025013.

Schweitzer, P. A. (2003). *Metallic materials: physical, mechanical, and corrosion properties*. CRC Press.

Schwenk, W. (1964). Theory of stainless steel pitting. *Corrosion*, *20*(4), 129t-137t.

Seeley, T. D. (2009). *The wisdom of the hive: the social physiology of honey bee colonies*. Harvard University Press.

Sergeev, G. B. (2003). Cryochemistry of metal nanoparticles. *Journal of Nanoparticle Research*, *5*(5-6), 529-537.

Sergeev, G. B. (2006). *Nanochemistry*. Elsevier.

Shahryari, A., and Omanovic, S. (2007). Improvement of pitting corrosion resistance of a biomedical grade 316LVM stainless steel by electrochemical modification of the passive film semiconducting properties. *Electrochemistry communications*, *9*(1), 76-82.

Shankar, S. S., Rai, A., Ahmad, A., and Sastry, M. (2004). Rapid synthesis of Au, Ag, and bimetallic Au core–Ag shell nanoparticles using Neem (Azadirachta indica) leaf broth. *Journal of colloid and interface science*, *275*(2), 496-502.

Sharman, C. F. (1944). Filiform underfilm corrosion of lacquered steel surfaces. Nature, 153(3890), 621.

Shaw, H. (1962). *The corrosion of zinc-stainless steel couples in flowing sea water* (Doctoral dissertation, Newark College of Engineering).

Shchukin, D. G., Zheludkevich, M., Yasakau, K., Lamaka, S., Ferreira, M. G., and Möhwald, H. (2006). Layer-by-layer assembled nanocontainers for self-healing corrosion protection. *Advanced Materials*, *18*(13), 1672-1678.

Shervani, Z., and Yamamoto, Y. (2011). Carbohydrate-directed synthesis of silver and gold nanoparticles: effect of the structure of carbohydrates and reducing agents on the size and morphology of the composites. *Carbohydrate research*, *346*(5), 651-658.

Shi, X. (2010). On the use of nanotechnology to manage steel corrosion. *Recent Patents on Engineering*, *4*(1), 44-50.

Shih, C. C., Shih, C. M., Su, Y. Y., Su, L. H. J., Chang, M. S., and Lin, S. J. (2004). Effect of surface oxide properties on corrosion resistance of 316L stainless steel for biomedical applications. *Corrosion Science*, *46*(2), 427-441.

Shrivastava, S., Bera, T., Roy, A., Singh, G., Ramachandrarao, P., and Dash, D. (2007). Characterization of enhanced antibacterial effects of novel silver nanoparticles. *Nanotechnology*, *18*(22), 225103.

Singh, N., Singh, J., Kaur, L., Sodhi, N. S., and Gill, B. S. (2003). Morphological, thermal and rheological properties of starches from different botanical sources. *Food chemistry*, *81*(2), 219-231.

Singh, A. K., and Quraishi, M. A. (2010). Inhibiting effects of 5-substituted isatin-based Mannich bases on the corrosion of mild steel in hydrochloric acid solution. *Journal of Applied Electrochemistry*, *40*(7), 1293-1306.

Singh, R., Wagh, P., Wadhwani, S., Gaidhani, S., Kumbhar, A., Bellare, J., and Chopade, B. A. (2013). Synthesis, optimization, and characterization of silver nanoparticles from Acinetobacter calcoaceticus and their enhanced antibacterial activity when combined with antibiotics. *International Journal of Nanomedicine*, *8*, 4277.

Solomon, M. M., and Umoren, S. A. (2016). In-situ preparation, characterization and

anticorrosion property of polypropylene glycol/silver nanoparticles composite for mild steel corrosion in acid solution. *Journal of colloid and interface science*, *462*, 29-41.

Sosa, I. O., Noguez, C., and Barrera, R. G. (2003). Optical properties of metal nanoparticles with arbitrary shapes. *The Journal of Physical Chemistry B*, *107*(26), 6269-6275.

Stratmann, M., and Streckel, H. (1990). On the atmospheric corrosion of metals which are covered with thin electrolyte layers—I. Verification of the experimental technique. *Corrosion Science*, *30*(6-7), 681-696.

Sun, S., Murray, C. B., Weller, D., Folks, L., and Moser, A. (2000). Monodisperse FePt nanoparticles and ferromagnetic FePt nanocrystal superlattices. *science*, *287*(5460), 1989-1992.

Sweeney, A. E., Seal, S., and Vaidyanathan, P. (2003). The promises and perils of nanoscience and nanotechnology: Exploring emerging social and ethical issues. *Bulletin of Science, Technology and Society*, *23*(4), 236-245.

Szklarska-Smialowska, Z. (1986). Pitting corrosion of metals. *National Association of Corrosion Engineers, 1440 South Creep Drive, Houston, Texas 77084, USA, 1986. 431*.

Takeda, Y., Hizukuri, S., and Juliano, B. O. (1986). Purification and structure of amylose from rice starch. *Carbohydrate research*, *148*(2), 299-308.

Tran-Quang. H., and Le, A. T. (2013). Silver nanoparticles: synthesis, properties, toxicology, applications and perspectives. *Advances in Natural Sciences: Nanoscience and Nanotechnology*, *4*(3), 033001.

Uthumporn, U., Shariffa, Y. N., and Karim, A. A. (2012). Hydrolysis of native and heat-treated starches at sub-gelatinization temperature using granular starch hydrolyzing enzyme. *Applied biochemistry and biotechnology*, *166*(5), 1167-1182.

Venu, R., Ramulu, T. S., Anandakumar, S., Rani, V. S., and Kim, C. G. (2011). Bio-directed synthesis of platinum nanoparticles using aqueous honey solutions and their catalytic applications. *Colloids and Surfaces A: Physicochemical and Engineering Aspects*, *384*(1-3), 733-738.

Vigneshwaran, N., Nachane, R. P., Balasubramanya, R. H., and Varadarajan, P. V. (2006). A novel one-pot 'green'synthesis of stable silver nanoparticles using soluble starch. *Carbohydrate research*, *341*(12), 2012-2018.

Vijayakumar, M., Priya, K., Nancy, F. T., Noorlidah, A., and Ahmed, A. B. A. (2013). Biosynthesis, characterisation and anti-bacterial effect of plant-mediated silver nanoparticles using Artemisia nilagirica. *Industrial Crops and Products*, *41*, 235-240.

Vilchis-Nestor, A. R., Sánchez-Mendieta, V., Camacho-López, M. A., Gómez-Espinosa, R. M., Camacho-López, M. A., and Arenas-Alatorre, J. A. (2008). Solventless synthesis and optical properties of Au and Ag nanoparticles using Camellia sinensis extract. *Materials Letters*, *62*(17-18), 3103-3105.

Wahdan, H. A. L. (1998). Causes of the antimicrobial activity of honey. *Infection*, *26*(1), 26-31.

Warheit, D. B., Sayes, C. M., Reed, K. L., and Swain, K. A. (2008). Health effects related to nanoparticle exposures: environmental, health and safety considerations for assessing hazards and risks. *Pharmacology and therapeutics*, *120*(1), 35-42.

Wei, L., Lu, J., Xu, H., Patel, A., Chen, Z. S., and Chen, G. (2015). Silver nanoparticles: synthesis, properties, and therapeutic applications. *Drug Discovery Today*, *20*(5), 595-601.

Wilmott, M. J., and Jack, T. R. (2000). Corrosion by soils. *Uhlig's Corrosion Handbook, John Wiley and Sons Inc., New York*, 329-348.

Xia, T., Li, N., and Nel, A. E. (2009). Potential health impact of nanoparticles. *Annual review of public health*, *30*, 137-150.

Xia, Y., and Sun, Y. (2009). *U.S. Patent No. 7,585,349*. Washington, DC: U.S. Patent and Trademark Office.

Yakout, S.M.,and Mostafa, A.A. (2015) A novel green synthesis of silver nanoparticles using soluble starch and its antibacterial activity. *International Journal of Clinical and Experimental Medicine*. 8(3): 3583-3585

Yao, H. B., Li, Y., and Wee, A. T. S. (2000). An XPS investigation of the oxidation/corrosion of melt-spun Mg. *Applied Surface Science*, *158*(1-2), 112-119.

Yoosaf, K., Ipe, B. I., Suresh, C. H., and Thomas, K. G. (2007). In situ synthesis of metal nanoparticles and selective naked-eye detection of lead ions from aqueous media. *The Journal of Physical Chemistry C*, *111*(34), 12839-12847.

Zhang, J. P., Chen, P., Sun, C. H., and Hu, X. J. (2004). Sonochemical synthesis of colloidal silver catalysts for reduction of complexing silver in DTR system. *Applied Catalysis A: General*, *266*(1), 49-54.

Zhang, X. F., Liu, Z. G., Shen, W., and Gurunathan, S. (2016). Silver nanoparticles: synthesis, characterization, properties, applications, and therapeutic approaches. *International journal of molecular sciences*, *17*(9), 1534.

Zhou, Y. G., Rees, N. V., and Compton, R. G. (2011). The electrochemical detection and characterization of silver nanoparticles in aqueous solution. *Angewandte Chemie*, *123*(18), 4305-4307.

Zobel, H. F. (1988). Molecules to granules: a comprehensive starch review. *Starch-Stärke*, *40*(2), 44-50.

Zobel, H. F., Young, S. N., and Rocca, L. A. (1988). Starch gelatinization: An X-ray diffraction study. *Cereal Chem*, *65*(6), 443-446.

APPENDIX

1: Procedures for Reagent Preparation

a) To prepare 0.5 M HCl, the product of the specific gravity (SG) and percentage purity (%) of the compound determined the mass concentration. Since the SG and percentage purity are 1.18 and 36% respectively, the Mass concentration will be 1.18 x 0.36

Therefore, the Mass conc. = 0.4248 gcm^{-3}

However, Mass Conc. in gdm^{-3};

If 0.4248 g = 1 cm^3

X g = 1000 cm^3

Thus, X = 0.4248 g x 1000 cm^3 = 424.8 gdm^{-3}

Given that, Molarity = $\frac{\text{Mass Conc}}{\text{Molar Mass}}$

Then, the Mass conc. (424.8 gdm^{-3}) by the Molar mass of HCl (36.5 $gmol^{-1}$) is:

$= \frac{424.8\ g/dm3}{36.5} = 11.64$ M

Furthermore, 250 cm^3 of 0.5 M HCl was prepared from stock of (11.64 M) as follows:

$C_1V_1 = C_2V_2$

Where, C_1 represents the initial conc., C_2 represents the final conc., V_1 represents the initial volume and V_2 represents the final volume.

i.e: C_1 = 11.64 M, V_1 =?, C_2 = 0.5 M, V_2 = 250 cm^3

By making the unknown V_1 the subject of the formula:

$V_1 = C_2 V_2 / C_1$

Therefore, the initial volume of HCl is:

$= \frac{0.5 \times 250}{11.64} = 10.74\ cm^3$

Therefore, 10.74 cm^3 of HCl in 250 cm3 of solution gives 0.5 M HCl.

Thus, 100 cm^3 of deionized water was put into a 250 cm^3 volumetric flask. Then, 10.74 cm^3 of HCl was added from the stock solution and the solution was made up to 250 cm^3 mark using deionized water.

b) Similarly, to prepare 0.1 M $AgNO_3$ having a Molar mass of 170 $gmol^{-1}$, the Mass conc. of the compound was ascertained by:

Mass Conc. in gdm^{-3} = Molarity x molar mass

That is, 0.1 mol/dm^3 x 170 $gmol^{-1}$ = 17 gdm^{-3}

So if, 17 g of $AgNO^3$ = 1000 cm^3 and

X g of $AgNO^3$ = 250 cm^3

Then, X g = $\frac{17 \times 250}{1000}$ = 4.25 g

Therefore, 4.25 g of $AgNO_3$ was dissolved in 50 cm^3 of deionized water in a 250 cm^3 volumetric flask, and was made up to mark.

2: Calculated Values of Corrosion Rate (mpy) and Inhibition Efficiency (%IE) for Mild Steel in 0.5 M HCl in the Absence and the Presence of Varied Concentration of starch at (30^oC, 40^oC, 50^oC, 60^oC and 70^oC) from Weight Loss Measurement

Starch-AgNPs Conc. (mg/L)	**Corrosion Rate (mpy)**					**Inhibition Efficiency (%IE)**				
	30^oC	**40^oC**	**50^oC**	**60^oC**	**70^oC**	**30^oC**	**40^oC**	**50^oC**	**60^oC**	**70^oC**
Blank	4.248	16.811	40.022	45.312	52.467	_	_	_	_	_
1	2.311	11.011	30.124	35.332	42.026	45.598	34.501	24.731	22.025	19.900
5	1.964	9.359	25.003	30.386	35.722	53.766	44.328	37.527	32.940	31.915
10	1.846	8.657	23.503	28.259	33.579	56.544	48.504	41.275	37.635	35.999
50	1.717	8.051	22.093	26.563	31.228	59.581	52.109	44.798	41.378	40.481
100	1.683	7.970	21.430	25.500	30.291	60.381	52.591	46.454	43.724	42.267
200	1.566	7.571	21.001	24.735	29.685	63.136	54.964	47.526	45.412	43.422
500	1.856	7.661	21.011	24.735	29.688	56.308	54.429	47.501	45.412	43.416

3: Calculated Values of Corrosion Rate (mpy) and Inhibition Efficiency (%IE) for Mild Steel in 0.5 M HCl in the Absence and the Presence of Varied Concentration of Starch with 5 cm^3 Honey at (30°C, 40°C, 50°C, 60°C and 70°C) from Weight Loss Measurement

Starch-AgNPs Conc. (Mg/L)	**Honey (cm^3)**	**Corrosion Rate (mpy)**					**Inhibition Efficiency (%IE)**				
		30°C	**40°C**	**50°C**	**60°C**	**70°C**	**30°C**	**40°C**	**50°C**	**60°C**	**70°C**
Blank	**Blank**	4.248	16.811	40.022	45.312	52.467	–	–	–	–	–
–	**5**	2.939	12.322	35.004	42.085	49.543	30.815	26.703	12.538	7.122	5.573
1	**5**	1.472	8.178	22.423	29.352	36.772	65.348	51.353	43.973	35.222	29.914
5	**5**	1.352	5.879	16.591	22.283	30.493	68.173	65.029	58.545	50.823	41.882
10	**5**	1.301	5.828	15.856	21.419	29.234	69.374	65.332	60.382	52.729	44.281
50	**5**	1.298	5.776	14.769	20.418	28.711	69.444	65.642	63.098	54.939	45.278
100	**5**	1.305	5.712	14.654	20.072	27.991	69.27 9	66.022	63.385	55.703	46.650
200	**5**	1.376	5.781	14.481	19.605	26.752	67.608	65.612	63.817	56.733	49.012
500	**5**	1.384	5.729	14.903	19.605	26.692	67.419	65.921	62.763	56.733	49.126

4: Synergism Parameter (S_1), for Mild Steel in 0.5 M HCl in the Absence and Presence of Varied Concentration of Starch-AgNPs with Honey at (30°C, 40°C, 50°C, 60°C and 70°C) from Weight Loss Measurement

Starch-AgNPs Conc. (mg/L)	**Honey (cm^3)**	**Synergism Parameter (Si)**				
		30°C	**40°C**	**50°C**	**60°C**	**70°C**
Blank	**Blank**	–	–	–	–	–
–	**5**	–	–	–	–	–
1	**5**	1.172	1.196	0.844	0.822	0.846
5	**5**	1.244	1.094	0.853	0.985	0.893
10	**5**	1.263	1.154	0.889	0.846	0.937
50	**5**	1.306	1.204	0.907	0.881	1.018
100	**5**	1.321	1.204	0.929	0.911	1.026
200	**5**	1.395	1.248	0.940	0.925	0.999
500	**5**	1.297	1.234	0.956	0.925	0.997

5: Adsorption Evaluation, for Mild Steel in 0.5 M HCl in the Presence of Varied Concentration of Starch-AgNPs at (30^oC, 40^oC, 50^oC, 60^oC and 70^oC) from Weight Loss Measurement

Starch-AgNPs Conc. (mg/L)	**Adsorption Parameters**				
	30^oC	**40^oC**	**50^oC**	**60^oC**	**70^oC**
1	0.456	0.345	0.247	0.220	0.199
5	0.538	0.443	0.375	0.329	0.319
10	0.565	0.485	0.413	0.376	0.359
50	0.596	0.521	0.448	0.414	0.405
100	0.604	0.526	0.465	0.437	0.423
200	0.631	0.549	0.475	0.454	0.434
500	0.563	0.544	0.475	0.454	0.434

6: Adsorption Evaluation, for Mild Steel in 0.5 M HCl in the Presence of Varied Concentration of Starch-AgNPs with Honey at (30^oC, 40^oC, 50^oC, 60^oC and 70^oC) from Weight Loss Measurement

Starch-AgNPs Conc. (mg/L)	**Honey (cm^3)**	**Adsorption Parameters**				
		30^oC	**40^oC**	**50^oC**	**60^oC**	**70^oC**
1	**5**	0.653	0.514	0.439	0.352	0.299
5	**5**	0.682	0.650	0.585	0.508	0.419
10	**5**	0.694	0.653	0.604	0.527	0.443
50	**5**	0.694	0.656	0.631	0.549	0.453
100	**5**	0.693	0.660	0.634	0.557	0.467
200	**5**	0.676	0.656	0.638	0.567	0.490
500	**5**	0.674	0.659	0.628	0.567	0.491

7: Calculated Values of Corrosion Rate (mpy) and Inhibition Efficiency (%IE) for Mild Steel in 0.5 M HCl in the Absence and the Presence of Varied Concentration of Honey at (30^oC, 40^oC, 50^oC, 60^oC and 70^oC) from Weight Loss Measurement

Honey (cm^3)	**Corrosion Rate (mpy)**					**Inhibition Efficiency (%IE)**				
	30^oC	**40^oC**	**50^oC**	**60^oC**	**70^oC**	**30^oC**	**40^oC**	**50^oC**	**60^oC**	**70^oC**
Blank	4.248	16.811	40.022	45.312	52.467	_	_	_	_	_
2	4.190	15.911	39.501	44.999	51.112	1.365	5.354	1.301	0.691	2.685
3	4.115	15.250	39.005	44.911	46.125	3.131	9.286	2.541	0.885	0.121
4	3.527	14.786	37.015	43.417	48.011	16.972	12.046	7.513	4.182	8.491
5	2.939	12.322	35.004	42.085	49.543	30.815	26.703	12.538	7.122	5.573
6	2.351	9.858	28.003	33.668	39.635	44.656	41.359	30.031	25.697	24.457